PEOPLE'S DEMOCRATIC REPUBLIC OF ALGERIA

MINISTRY OF HIGHER EDUCATION AND SCIENTIFIC RESEARCH

UNIVERSITY M'HAMED BOUGARA OF BOUMERDES

Faculty of Technology

Department of Electrical Systems Engineering

Master's thesis

Presented by

LUUTU STEPHEN GONZAGA

ALLAL CHERIF MOHAMED

Course: Electrical Engineering

Major: Electrical Machines

DESIGN AND IMPLEMENTATION OF A SOLAR PHOTOVOLTAIC WATER PUMPING SYSTEM

Defended publicly on 27/06/2024 in front of a jury composed of:

Mr. HACHEMI	Madjid	Professor	UMBB	President
Mr. KAOUANE	Mohamed	MCA	UMBB	Examiner
Ms. FELLAG	Ratiba	Senior Researcher	CDTA	Examiner
Mr. HAMEL	Meziane	MCA	UMBB	Supervisor
Mr. MOUALEK	Riad	PHD Student	UMMTO	Co-supervisor

University Year: 2023/2024

ABSTRACT

Abstract

This project focuses on developing a photovoltaic water pumping system (PVWPS) that harnesses solar energy to provide an efficient and eco-friendly solution for water management. We designed and implemented key components including a DC-DC boost converter and its support electronic cards using professional software. This system aims to convert a 30V DC input to a variable DC output, essential for powering one of the water fountains at our faculty at different water heads. Through meticulous integration of solar panels, MPPT controller, batteries, and load, our project demonstrates significant potential in sustainable water supply solutions. Theoretical insights and practical applications highlight our innovative approach to addressing real-world challenges in water access and power electronics.

Key words: Power Converters, PVWPS, MPPT, Solar Panels, Electronic Card Design.

ملخص

هذا المشروع يركز على تطوير نظام ضخ المياه الكهروضوئي (PVWPS) الذي يستعمل الطاقة الشمسية لتوفير حل فعال لضخ المياه وفي نفس الوقت صديق للبيئة، قمنا بتصميم وتصنيع العناصر الأساسية بما في ذلك محول رفع الجهد DC-DC والبطاقات الإلكترونية بإستخدام برامج وتقنيات إحترافية، يهدف هذا التصميم إلى تحويل توتر الدخل المقدر بقيمة 30 فولط DC إلى توتر مخرج بقيم متغيرة، وهذا لتشغيل أحد نوافير المياه لكلية التكنولوجيا في بومرداس. من خلال التصميم الدقيق لهذا المشروع الذي يحتوي على الألواح الشمسية، وحدة التحكمMPPT ، البطاريات والحمولة يوضح هذا المشروع إمكانات كبيرة في حلول المياه المستدامة. تسلّط الرؤى النظرية والتطبيقات العلمية الضوء على نهجنا المبتكر في مواجهة تحديات العالم الحقيقي في الوصول إلى المياه وإلكترونيات الطاقة.

الكلمات المفتاحية: محولات الطاقة، PVWPS, MPTT, ألواح شمسية، تصميم بطاقة إلكترونية.

Résumé

Ce projet est dédié au développement d'un système de pompage d'eau photovoltaïque (PVWPS) qui exploite l'énergie solaire pour fournir une solution efficace et écologique pour la gestion de l'eau. Nous avons conçu et mis en œuvre des composants clés, notamment un convertisseur élévateur DC-DC et ses cartes électroniques, à l'aide de logiciels professionnels. Ce système vise à convertir une entrée 30V DC en une sortie DC variable, essentielle pour alimenter l'une des fontaines de notre faculté à différentes hauteurs d'eau. A travers l'intégration méticuleuse des panneaux solaires, d'un contrôleur MPPT, des batteries et de la charge, ce projet démontre un potentiel important en matière de solutions durables d'approvisionnement en eau. Les

connaissances théoriques et les résultats pratiques mettent en évidence notre approche innovante pour relever les défis du monde réel en matière d'accès à l'eau et d'électronique de puissance.

Mots clés : Convertisseurs de Puissance, PVWPS, MPPT, Panneaux Solaires, Conception de Carte ÉlectroniquE

ACKNOWLEDGEMENTS

ACKNOWLEDGEMENTS

First and foremost, I thank God for His grace in enabling us to complete this work. I am deeply grateful to my family for their unwavering support, especially my parents and my only sister. I extend my heartfelt thanks to our professors, Meziane Hamel and Riad Moualek, for their invaluable guidance.

My sincere appreciation also goes to my partner, Stephen, for his significant contribution to this project. Lastly, I would like to thank myself for the effort and perseverance I have shown throughout this journey.

Allal Cherif Mohamed

I would like to express my profound gratitude to the Almighty God for His guidance and strength throughout this journey. I extend my heartfelt thanks to our supervisors, Riad Moualek and Meziane Hamel for their invaluable support and expertise, and to my binome Cherif for his collaboration.

This project was implemented at the faculty of technology UMBB. I would like to appreciate the University M'Hamed Bougara of Boumerdes for this wonderful opportunity and journey of growth in skills and knowledge, I'm forever grateful.

Additionally, I'm filled with gratitude to my entire family back home in Uganda, who have always supported me without fail in all circumstances throughout this enormous journey. In the same breath, I extend my heartfelt appreciation to all my friends for their moral support throughout my studies.

Lastly, I commend myself for the perseverance, hard work and dedication that made this achievement possible.

Luutu Stephen Gonzaga

TABLE OF CONTENTS

TABLE OF CONTENTS

CHAPTER III: DESIGN AND IMPLEMENTATION OF THE PVWPS

LIST OF FIGURES

LIST OF FIGURES

CHAPTER I: GENERALITIES ON PHOTOVOLTAIC WATER PUMPING SYSTEMS

CHAPTER II: POWER CONVERTERS FOR PHOTOVOLTAIC WATER PUMPING SYSTEMS

CHAPTER III: DESIGN AND IMPLEMENTATION OF THE PVWPS

APPENDICES

LIST OF TABLES

LIST OF TABLES

CHAPTER III: DESIGN AND SIMULATION OF PVWPS

ABBREVIATIONS

ABBREVIATIONS

AC	Alternating Current
CSI	Current source inverter
DC	Direct Current
DG	Diesel generator
GPH	Gallons Per Hour
GPM	Gallons Per Minute
GTO	Gate turn-off
HC	Hill Climbing
HP	Horse power
I/O	Input and Output
LR	Load Regulation
MCT	MOS-controlled thyristor
MLPT	Minimum Losses Point Tracking
MPPT	Maximum Power Point Tracking
MPP	Maximum Power Point
PCB	Printed Circuit Board
P&O	Perturb and Observe
PV	Photovoltaic
PVWPS	Photovoltaic Water Pumping Systems
PWM	Pulse Width Modulation
RMS	Root mean square
SCR	Silicon controlled rectifier
UMBB	University M'Hamed Bougara of Boumerdes
VSI	Voltage source inverter

LIST OF SYMBOLS AND VARIABLES

LIST OF SYMBOLS AND VARIABLES

Ve	Input voltage
Ie	Input current
Pe	Input power
Vs	Output voltage
Is	Output current
Ps	Output power
Cste	Constant
α	Duty cycle
ΔV	Voltage ripples
ΔI	Current ripples
f	Frequency
I_L	Inductor current
V_L	Inductor voltage
U_{FL}	Full load terminal voltage
U_{NL}	No load terminal voltage
LR	Load Regulator
Lmin	The minimal inductor value
Cmin	The minimal capacitor value
Vt	Triangular signal
Vref	Sinusoidal reference signal
Un	Nominal voltage

GENERAL INTRODUCTION

GENERAL INTRODUCTION

Photovoltaic Water Pumping Systems (PVWPS) are increasingly gaining attention and application due to their sustainable and efficient approach to water management. PVWPS utilize solar energy to power water pumps, converting sunlight directly into electrical energy through photovoltaic (PV) panels. This renewable energy system is particularly advantageous in remote and off-grid areas where conventional electricity supply is unavailable or unreliable. The growth of PVWPS in recent years can be attributed to advancements in solar technology, decreasing costs of PV panels, and a heightened global emphasis on reducing carbon footprints. The advantages of PVWPS include minimal operational costs, low maintenance requirements, and the ability to provide a consistent water supply without relying on fossil fuels, making them an environmentally friendly and economically viable solution for agricultural, industrial, and domestic water needs.

Electronic power converters play a crucial role in the constitution of Photovoltaic Water Pumping Systems (PVWPS). These converters are responsible for managing and optimizing the electrical energy generated by the PV panels, ensuring that the power supplied to the water pumps is stable and efficient. The importance of electronic power converters lies in their ability to convert the direct current (DC) produced by the solar panels into the alternating current (AC) required by many water pump motors or to manage the DC-DC conversion for DC pump motors.

DC-DC conversion is particularly vital for PVWPS that utilize DC pump motors, with DC-DC booster converters playing a key role in this process. DC-DC boosters increase the voltage from the PV panels to a level suitable for the DC pump motors, ensuring that the pump operates efficiently even when the solar input is variable.

In this project, we design and implement a DC-DC boost converter along with its supporting electronic cards, specifically the control card and power supply card, entirely from scratch. The development process involves the use of various software tools, including Altium Designer for PCB design, Proteus 8 Professional for circuit simulation, MikroC for microcontroller programming, and MATLAB/Simulink for system modeling and analysis. The process involved meticulous planning and execution to ensure all components functioned seamlessly together. Our approach integrated both hardware and software elements to create a robust and efficient system.

This comprehensive design and implementation project demonstrates our capability in developing complex electronic systems.

Chapter 1 provides an overview of PVWPS, including installation procedures, control mechanisms, and case studies conducted in Algeria. In Chapter 2, we delve into the crucial components of PVWPS, particularly power converters such as DC boosters and inverters, essential for converting and regulating the solar energy into usable power for the water pumping system. Finally, Chapter 3 details the implementation and design of our PVWPS, where we develop electronic cards and demonstrate the functionality by powering a water fountain at our faculty. Through these chapters, we aim to provide a comprehensive understanding of PVWPS technology and showcase its practical application in addressing water management challenges.

CHAPTER I

GENERALITIES ON PHOTOVOLTAIC WATER PUMPING SYSTEMS

I.1. Introduction

In the field of sustainable energy solutions, photovoltaic water pumping systems (PVWPS) stand out as a beacon of innovation and environmental stewardship. These systems harness the power of sunlight to efficiently pump water, offering a reliable and eco-friendly alternative to traditional pumping methods. Understanding the fundamentals of photovoltaic water pumping systems is essential for grasping their significance in various applications, from agriculture to rural development and beyond.

This chapter provides a comprehensive overview of PVWPS, delving into their functionality, types, design considerations, and control mechanisms. By exploring the intricate workings of these systems, we aim to unravel the complexities behind their operation and elucidate the principles driving their efficiency and effectiveness. From solar panels to pumping mechanisms, this chapter elucidates the core components of photovoltaic water pumping systems, shedding light on their transformative potential in addressing water access challenges worldwide.

I.2. Types of photovoltaic water pumping systems

PVWPS are classified depending on the configuration of the systems. There are two configurations of PV water pumping systems:

I.2.1. Hybrid systems

These combine multiple energy sources, usually two sources, such as wind turbines, diesel generators, or photovoltaic panels to ensure a continuous and reliable power supply. This approach allows flexibility to adapt to different energy requirements and environmental conditions. For example, during periods of low wind or sunlight, a diesel generator can kick in to provide additional power, ensuring an uninterrupted electricity supply. Likewise, excess energy generated by renewable energy sources during favorable conditions can be stored for later use or fed back to the grid. By combining different energy sources, hybrid systems provide a sustainable and flexible solution to meet diverse energy needs while reducing dependence on fossil fuels.

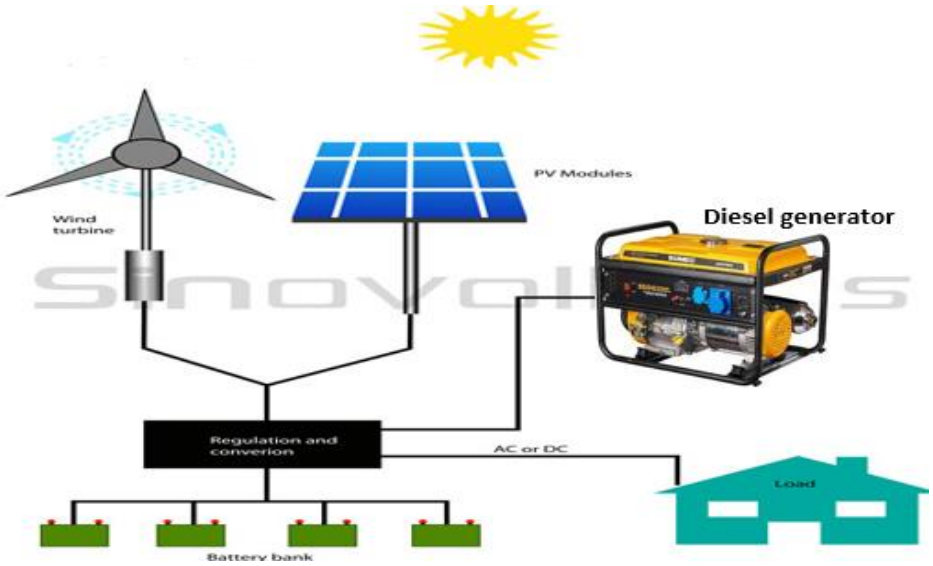

Fig I.1. Hybrid PVWPS system

I.2.2. Standalone systems

The AC standalone water pumping systems in general consist of a PV array, an inverter with a centralized maximum power point tracker (MPPT), and a pump. Such a system can have a block of batteries as a backup power supply, but because the system cost is a very important factor, systems are designed in a way to meet the demand during the solar day without any need for batteries.

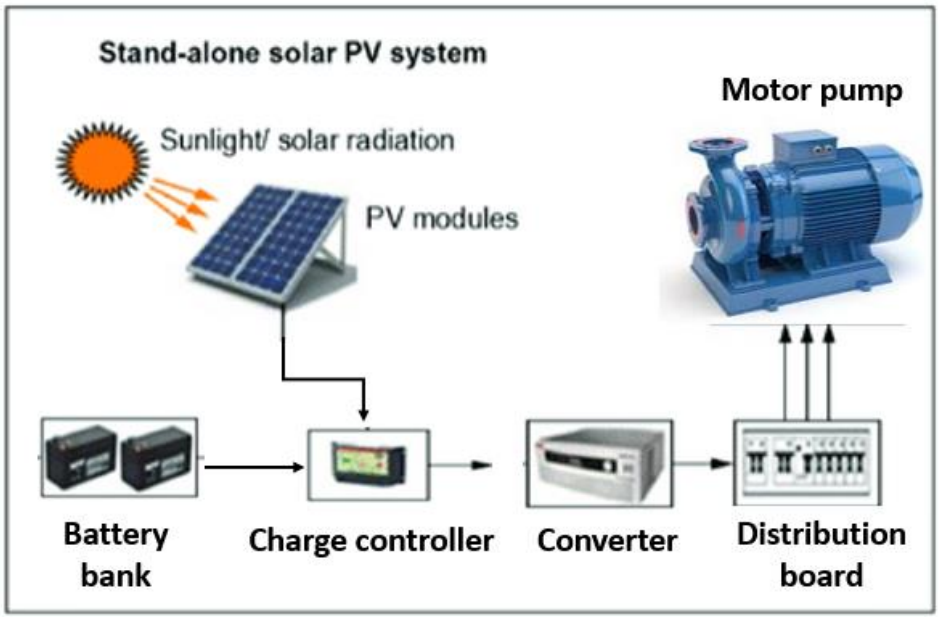

Fig I.2. Standalone PVWPS system

We will detail more about this system because it is the one that our project is about although in our system, we have a block of two batteries in series as backup.

I.3. Installation of photovoltaic water pumping system

Numerous failures in PVWPS stem from issues with the pump itself, despite the PV power supply boasting higher reliability than the pump/motor subsystem. Ensuring proper installation of the pumping hardware is crucial for enhancing reliability. Below are key considerations to bear in mind:

- Managing water level variations:

Wells can experience fluctuations in water levels seasonally, daily, or even hourly, with reports of drops up to 75 feet during pumping in rocky areas. To mitigate risks, pumps must be positioned to maintain the water inlet below the water level consistently. Incorporating a level switch or mechanical valve is advisable if the well's replenishment rate is lower than the maximum pumping rate to safeguard the pump from operating dry. Additionally, using float switches on storage tanks smaller than the daily pump rate can prevent water wastage or pump damage from overheating.

- Shielding the pump input:

Pump failure often results from sand intake. Employing a sand screen, available as an option from most pump manufacturers or through recommended methods, is crucial for wells susceptible to dirt and sand ingress.

- Grounding the equipment:

Water pumps are susceptible to lightning strikes due to their excellent grounding. It's advisable to avoid locating the pump system on elevated terrain and consider installing lightning rods nearby. Properly grounding the pump motor, array frame, equipment boxes, and one system conductor to the well casing or a bare conductor leading to the water level is essential. Avoid using the pump pipe string as a ground to prevent interruption during maintenance. Installing monitors for electronic protection is recommended in lightning-prone areas.

- Minimizing long pipe runs:

Extensive pipe runs, especially in wells with jack pumps, can result in significant losses. Friction losses, contingent on pump maintenance, pipe size, length, ammeter size, and pump cylinder bends, must be managed, particularly as PV system output varies throughout the day. Keeping friction losses below 10% of the head is critical to maintaining pump system efficiency, achieved through measures like oversizing pipes, reducing bends and junctions, and lowering flow rates.

- Safeguarding control equipment:

Housing all electronic control equipment in weather-resistant enclosures and using approved outdoor wires or conduits is imperative. Employing cables suitable for submersible pumps according to manufacturer recommendations is essential.

- Utilizing steel pipe:

Steel pipe is recommended for well usage, particularly with submersible pumps, due to its durability compared to plastic pipe which may break. However, plastic pipe offers a cost-effective means for water conveyance from the well to storage tanks or end users.

- Protecting the well:

Installing sanitary well seals for all wells and burying pipes at a depth that prevents damage from traffic, future trenching, or excavation is essential. Marking pipe runs for future reference aids in maintenance and identification.

I.4. Photovoltaic water pumping system design procedures

The high initial cost of a PV array is a significant drawback of PVWPS. Consequently, many researchers are focusing on determining the optimal size of a PV array, as well as other components such as the storage unit and inverter, to meet the required load at minimum cost. In general, three main methods are used for sizing PV systems: intuitive, numerical, and analytical [1, 2].

The simplest method is the intuitive approach, which relies on the worst month or the average monthly solar radiation for sizing the PV array and storage units. However, this method

may lead to over- or under sizing of the PV system, increasing costs or compromising system reliability, as noted by [3]. Therefore, it is primarily suitable for estimating initial and approximate sizes of a PV system [4].

On the other hand, the numerical method involves using hourly meteorological data to simulate the system's hourly energy flow, identifying possible system configurations that achieve a specific level of reliability. However, the main drawback is the lengthy computation time required to identify the optimal configuration within the design space, as it evaluates system reliability for all configurations [4].

In the analytical method, equations for PV system size in terms of system reliability are developed and utilized. Although this method offers simplicity and accuracy in calculating system size, the complexity of deriving equations' coefficients poses a challenge.

Nevertheless, several considerations must be addressed when sizing a PVWPS, including accurate information regarding water flow rate profile demand, the efficiency and specifications of PVWPS components, and other relevant factors [5].

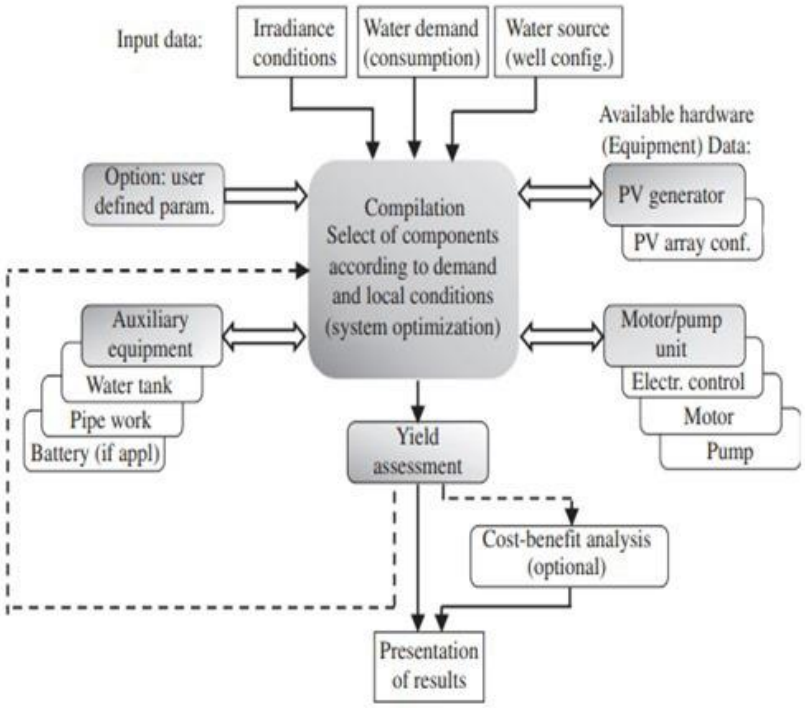

Fig I.3. Design parameters of a PV-water pumping system

I.5. Control procedures of PVWPS

Optimal control of a Photovoltaic Pumping System (PVWPS) is crucial for ensuring its efficient operation and overall reliability. Researchers have developed various control approaches to enhance the performance of PVWPS [6–12], encompassing MPPT algorithms, voltage regulation, frequency control, and load matching.

MPPT, a technique applied to PV systems, is designed to extract and track the maximum power generated by the PV array under different weather conditions. MPPT algorithms are categorized into conventional algorithms, typically effective in the absence of shading objectives, and algorithms based on stochastic and AI techniques. Conventional algorithms may encounter challenges in tracking the Maximum Power Point (MPP) under partial shading conditions and rapidly changing solar radiation [13]. Common conventional MPPT algorithms include Perturb and Observe (P&O), Incremental and Conductance (InCond), Hill Climbing (HC), Fractional V_{oc}, Fractional I_{sc}, Ripple Correlation Control, and Load Current or Load Voltage Maximization. Among these, P&O and InCond algorithms are widely utilized in PV systems [13]. The P&O algorithm involves perturbing the output voltage of a PV array with a small value, and the sign of the next perturbation value is determined based on the direction of change in PV power. Meanwhile, in the InCond algorithm, the PV voltage is adjusted by comparing the instantaneous conductance (I/V) with the incremental conductance ($\triangle I/\triangle V$).

In reference [14], the InCond method is employed to track the MPP of the PV array within a PVWPS, incorporating Minimum Losses Point Tracking (MLPT) for the induction motor. This proposed control strategy has demonstrated enhancements in the system's efficiency and a reduction in motor losses. Experimental findings have shown that implementing this strategy has resulted in a significant saving of 8% of the input power by mitigating motor losses. The basic principle behind this concept is to operate the motor with reduced flux when at reduced load torque, so that its efficiency is always maximum.

In Reference [15], an MPPT algorithm and sun-tracking algorithm were implemented to enhance the overall efficiency of a PVWPS operating within a range of different total heads, from 5 to 35 meters. The MPPT technique described in [15] is based on comparing the measured voltage of the PV array with a reference voltage, which corresponds to the voltage at which maximum power is achieved. This comparison is made against a sawtooth signal using a comparator, which

then generates a switching signal to control a MOSFET switch. The duty cycle of the triggering signal is determined by the output voltage of the PV array and the nature of the load. Additionally, the proposed sun tracker for the PVWPS led to a remarkable increase of 36% in the PV output power.

In Reference [16], two P&O-based MPPT approaches are introduced for PVWPS: the direct duty cycle-based P&O and the reference voltage-based P&O. The study investigates the impact of the algorithm's parameters, such as step size and perturbation rate, on the system's performance. Additionally, the advantages and drawbacks of each approach under varying weather conditions are analyzed. The findings reveal that the reference voltage perturbation method exhibits a quicker response compared to the direct duty ratio perturbation method when faced with rapidly changing solar radiation and temperature. Conversely, the stability characteristics of the direct duty ratio perturbation method surpass those of the reference voltage perturbation technique, especially with high perturbation rates. Furthermore, the direct duty cycle ratio perturbation technique demonstrates higher energy utilization efficiency than the reference voltage perturbation method for both gradual and rapid changes in solar radiation.

I.6. Motor pumps in PV pumping systems

Motor-pump sets in PVWPS are classified into two types: alternating current (AC) and direct current (DC), each with its own range of applications and motor characteristics. Both rotating and displacement pumps can be powered by AC or DC motors. Commonly used in PV pumping applications are DC permanent magnet motors (both brushed and brushless) and squirrel cage induction motors. The selection of motor types depends on size requirements and the nature of the water source. Factors like efficiency, availability, and price play a role in motor selection, with power demand being a crucial parameter. For instance, DC permanent magnet motors are suitable for 3 HP mechanical loads, while DC wound field motors are used for 3–10 HP, and AC induction motors are preferred for power demands exceeding 10 HP. Generally, DC motors exhibit higher efficiency than AC motors, and they do not require an inverter since PV arrays generate DC power. However, DC motors may need periodic replacement due to mechanical parts like the commutator, typically after 2000–4000 hours. In contrast, AC motors are cost-effective and are chosen for high power demands.

The types of motors used in photovoltaic water pumping systems are illustrated in the accompanying figure.

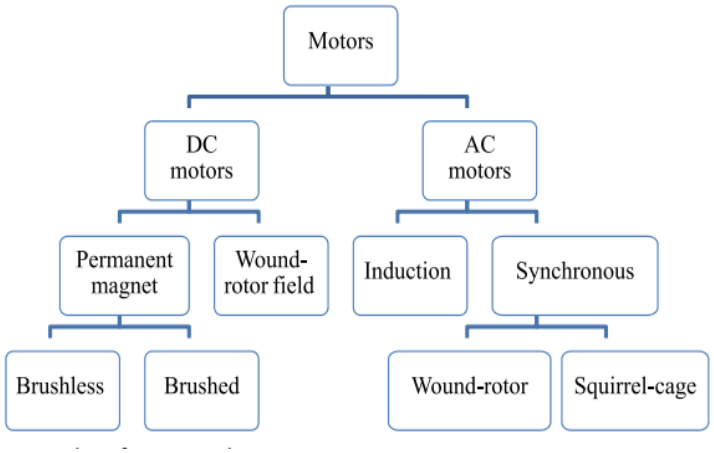

Fig I.4. Types of motors

I.7. Types of pumps

There are two broad categories of pumps used in standalone PV systems around the world: rotating and positive displacement. There are many variations on the designs of these two basic types [17].

I.7.1. Rotating pumps

Examples of the rotating pump types are centrifugal (fig I.5), rotating vane or screw drive. These pumps move water continuously when power is presented to the pump.

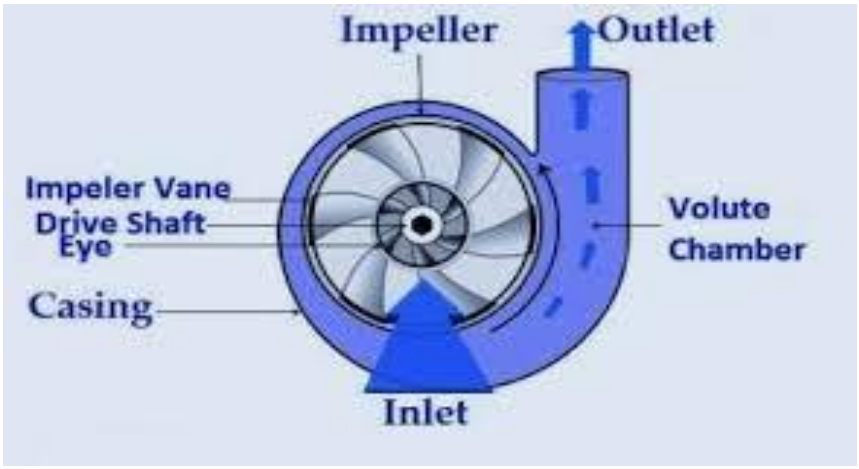

Fig I.5. A centrifugal pump

The performance of these pumps relies on factors such as head, solar radiation (which determines current output), and operating voltage. They are particularly suitable for extracting water from shallow reservoirs or cisterns. While they can be directly connected to the output of a PV array, their efficiency can be enhanced by employing an electronic controller, such as a linear current booster, to optimize the match between the pump and the PV array.

I.7.2. Positive displacement pumps

Positive displacement pumps, which transport water in discrete "packets," include diaphragm pumps and piston pumps (referred to as jack pumps), fig I.6. These pumps are commonly utilized for drawing water from deep wells. Their output is largely unaffected by pumping head and is directly proportional to solar radiation.

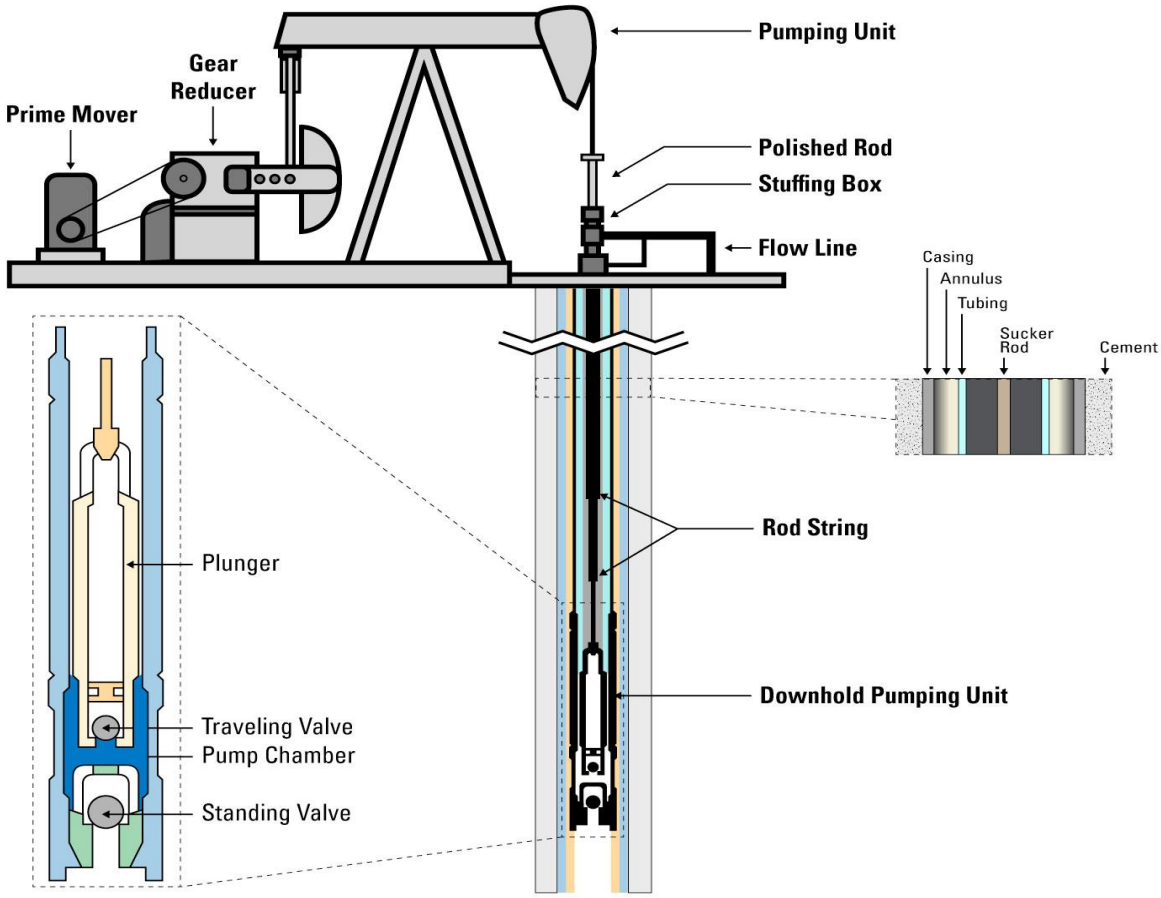

Fig I.6. A jack pump

Jack pumps should not be directly linked to a PV array output due to significant fluctuations in load current during each pump cycle. Peak power controllers are generally recommended to regulate this. These controllers adjust the operating parameters of the PV array to maximize current during motor starting and maintain optimal power conditions during operation. In some instances, batteries are integrated between the jack pump and the array to provide a stable voltage source for pump initiation and operation. Typically, these batteries are not sized to support nighttime pumping but rather to ensure stable system functioning.

Pumps are categorized as either surface or submersible. Surface pumps offer easier accessibility for maintenance. When selecting a surface pump, it is important to differentiate between suction and lift capacities. The maximum length of the pipe connecting the pump to the water source is determined by the pump's suction capability, while the pump's lift capability determines the elevation to which it can transport water to a storage tank.

Most submersible pumps boast high lift capabilities but are susceptible to damage from dirt and sand in the water. They should not be operated when the water level drops below the pump. The choice of pump type depends on factors such as required water volume, total dynamic head, and characteristics of the water source.

Ultimately, choosing the appropriate pump depends on various factors, including daily water requirements, water source, and pumping head. Volumetric pumps are suitable for water flow under 15m^3/day and pumping heads between 30 and 150m, while submersible centrifugal pumps are effective for high flow rates (25–100m^3/day) and medium pumping heads (10–30m).

I.8. Fountain pumps

Fountain pumps are created to deliver water flow for decorative and aeration fountain purposes in various settings, including residential, commercial, and industrial applications. These pumps can be adapted for indoor or outdoor use, with distinctions based on factors like pool or pond size and whether the purpose is decorative or functional. Certain fountain pumps are solar-powered, and they can collaborate with well pumps to craft unique garden or landscape features, like enchanting waterfalls. Fig I.7 shows a photo of an exterior decorative water fountain

Fig I.7. An exterior decorative water fountain

I.8.1. Types of Fountain Pumps

Fountain pumps can be classified into types based on a number of factors: operating method, application, and whether the pump is external or submersible.

- **Operation**

All pumps are designed based on either the dynamic or positive displacement principle. Dynamic pumps, such as centrifugal pumps, rely on fluid momentum and velocity to create pump pressure, while positive displacement pumps use expanding and contracting cavities to displace fluids. Dynamic pumps are suitable for generating variable flows, making them ideal for high flow rates with low viscosity fluids. In contrast, positive displacement pumps are apt for producing constant flows, making them effective for generating high pressures (and low flow rates) with high viscosity fluids.

Fountain pumps, commonly centrifugal pumps, employ the centrifugal force generated by an impeller's movement to move water through pressure. Functioning akin to a sump pump, a fountain pump redirects water back into the pond or reservoir rather than expelling it. Specifically, the pump transports water to an aerator or fountain device, creating a spray effect on the water's surface. The cascading water absorbs oxygen as it returns, facilitating aeration and supporting microbial

processes in wastewater breakdown or providing essential oxygenation for fish in ponds or farming tanks.

- **Application**

Fountain pumps serve distinct purposes, categorized into two main applications: commercial and industrial.

Commercial fountain pumps primarily contribute to decorative functions and are available in various configurations, designed for both indoor and outdoor settings. These pumps are commonly used in tabletop or garden fountains where the machinery is housed in an above-ground reservoir rather than a pond.

- Indoor pumps are tailored for smaller indoor fountains and decorative devices, typically featuring lower flow rates.
- Outdoor fountain pumps can handle a significantly higher water volume per hour compared to their indoor counterparts. They are employed for aesthetic purposes in outdoor fountain fixtures, as well as for aeration in pools and ponds.

Industrial fountain pumps serve broader applications, such as aerating wastewater from manufacturing processes, sewage treatment, or municipal water treatment. Additionally, these pumps play a role in circulating stagnant water to prevent algae buildup or control mosquito populations. Industrial pumps are generally more robust, designed to provide higher flow rates and pressures for various media.

- **Placement location**

Fountain pumps can be either submersible or external.

***Submersible** pumps have the pump motor sealed within the pump body, allowing the entire system to be submerged in the water source. They are easier to install and are typically more cost-effective. A submersible pump setup may look something like this (fig I.8), with a filter in place above the pump to prevent clogging

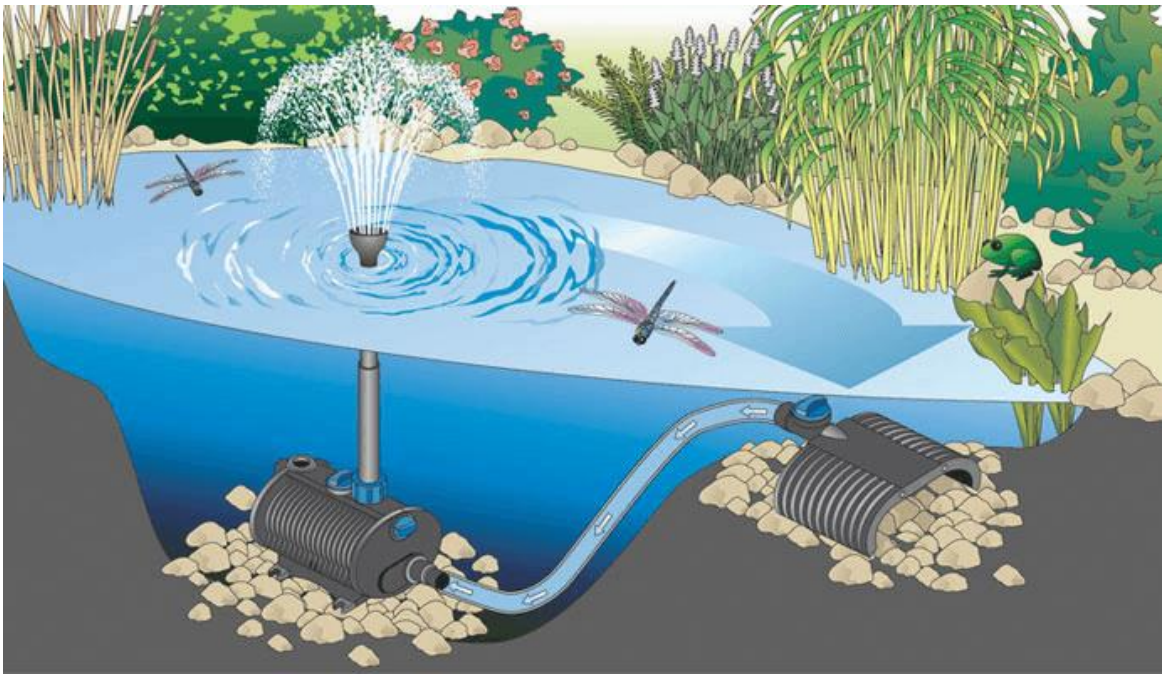

Fig I.8. A submersible pump with filters

* **External** pumps may require a more complex setup but are generally more efficient. They are well-suited for larger ponds, offering lower operating costs. External pumps are preferable for handling the back pressure associated with pressurized external filters, and they are easier to clean, repair, and tend to have a longer lifespan.

I.8.2. Specifications

Key specifications to consider when selecting fountain pumps include flow rate, pump head, pressure, horsepower, power rating, and outlet diameter.

- **Flow rate** denotes the volume discharge rate through the pump, usually expressed in gallons per minute (gpm) or gallons per hour (gph).

- **Pump head** defines the energy supplied to the liquid by the pump, often specified as a column height of liquid in feet.

- **Pressure** indicates the operational pressure of the pump, commonly given in pounds per square inch (psi) or bar.

- **Horsepower** measures the output power of the pump.

- **Power rating** signifies the power required to operate the pump, expressed in Watts (W) or horsepower (hp).

- **Outlet diameter** refers to the size of the pump's discharge or outlet connection, detailing the inner and outer diameter dimensions.

I.8.3. Matching Pump Specifications to the Application

Fountain pumps must be sized to fit the needs of the fountain, reservoir, or pond they are servicing. Considerations include:

Turning- To "turn" the water in a reservoir means to cycle all of the water through the pump. Sizing the pump to the desired turning rate is important for providing proper aeration.

Selection Tip: For ponds with a pressurized filter, turn the water every two hours (for a 2000-gallon reservoir, a 1000 gph pump is needed). For most other types of ponds, turn the water every hour (2000-gallon reservoir requires a 2000 gph pump).

Pipe sizing - Pipes and tubes must fit the pump and allow proper flow. Pipe sizes that are too small will restrict flow, while pump sizes which are too large will result in an insufficient outlet velocity.

Total head - Specifying the pump head requires determining the total head (resistance) of the system. This is determined from a combination of factors, including friction and elevation. In the case of the setup pictured below, the total head would include the length of the pipe (friction head) and the difference in height between the two pond surfaces (elevation head) [18].

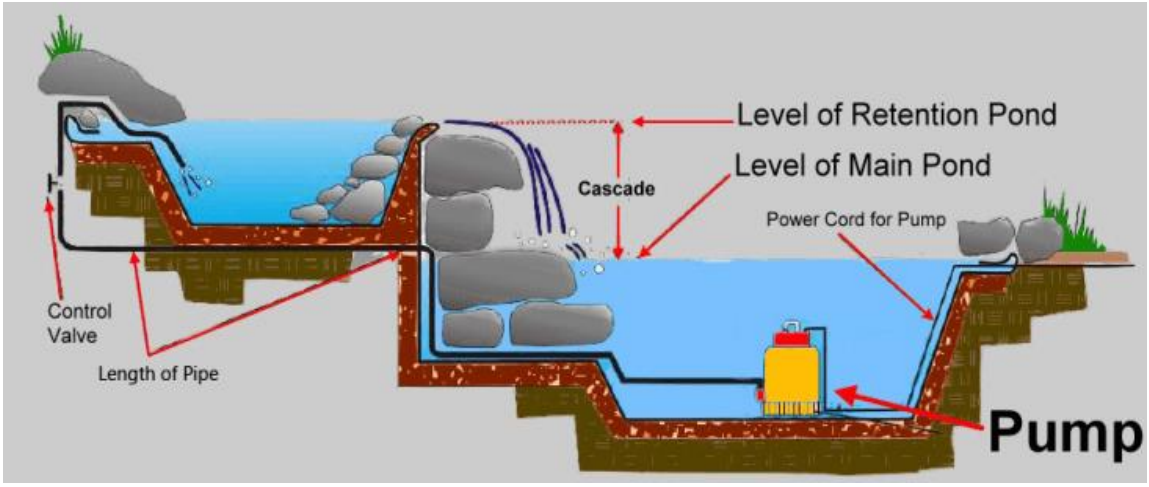

Fig I.9. Example of a water fountain set-up

I.9. Examples of PVWPS installations and their field Performance

In practice, the effectiveness of any PVWPS is influenced by various factors, encompassing meteorological conditions (such as solar radiation, ambient temperature, wind speed, humidity, and shadows), specifications of the PV modules (including conversion efficiency and tilt angle), and characteristics of the motor pump-hydraulic system (such as the I-V curve of the motor pump set, static, dynamic, and friction loss heads). This section provides an examination of PVWPS system reliability, feasibility, and field performance, drawing upon reported performances documented in the literature. A synthesis of these findings is subsequently presented, incorporating insights from the latest research articles on system performance.

An essential parameter for evaluating the viability of a PVWPS is the annual productivity rate, denoting the volume of pumped water per 1 kWp. Additionally, the efficiencies of the PV array, subsystem, and the overall system, including the performance factor (the ratio of field performance to theoretical performance), are critical metrics for assessing PVWPS feasibility. The yield factor (ratio of average daily pumped water to rated pumped water) and the capacity factor (ratio of actual annual pumped water to the annual pumped water at full rating) serve as other indicators to gauge the productivity of a PVWPS.

In a report conducted in Uganda, solar pumps are increasingly recognized as cost-effective, clean, and sustainable solutions for off-grid rural irrigation. With solar PV prices dramatically decreasing over the last decade, the International Renewable Energy Agency (IRENA) forecasts a 59% reduction in electricity costs from solar PV by 2025 compared to 2015 levels. Despite the higher initial costs of solar-powered irrigation systems (USD 1,000 to 3,000 per acre), they are more economical over their lifecycle than diesel pumps, which have lower initial but higher maintenance and fuel costs. Additionally, the overall system performance efficiency for solar pumps is reported to be in the range of 3%–10%. Solar pumps have zero fuel costs, are easier to maintain, and are less vulnerable to global price fluctuations, potentially reducing overall costs by 22-56% and achieving payback within two years.[19]

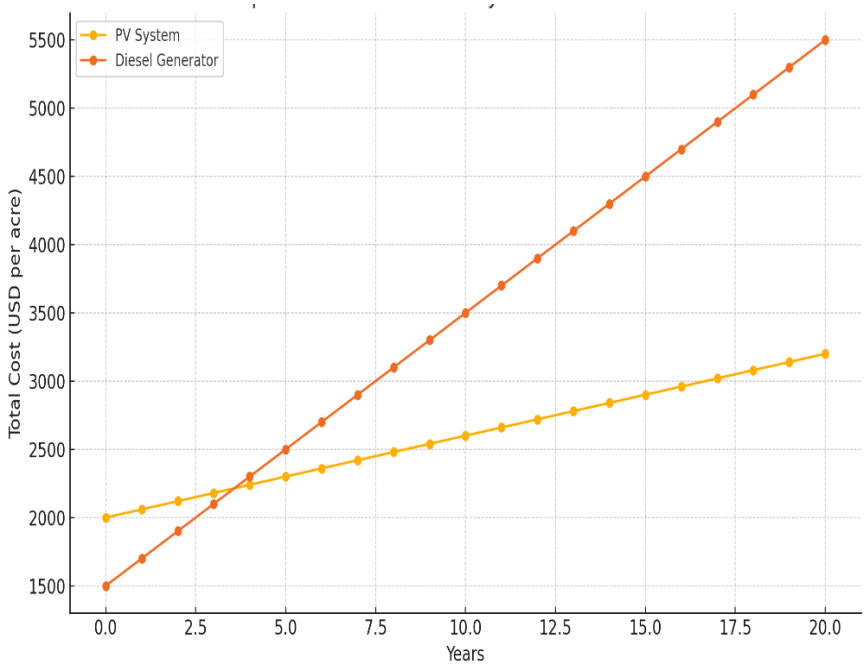

Fig. I.10. Overtime cost comparison of PVWPS and DG-based systems

In Reference [20], an assessment was conducted on the performance of several PVWPSs situated in four distinct wilayas in Algeria—Tamanrasset, Oran, Algiers, and Bechar. These PVWPSs exhibited variations in their hourly load demands, PV module types, PV array configurations, storage tank capacities, pumping heads, and pump types. The impact of load profiles was elucidated through a metric termed "relative deficit," representing the ratio of the total demand deficit to the overall demanded water. The findings reveal a direct correlation between the relative deficit and the pumping head, underscoring the influence of these factors on system performance. Moreover, the relative deficit value is found to be contingent on the storage tank capacity of the system. Notably, the PVWPS equipped with a multistage pump demonstrated superior performance, particularly in scenarios with high pumping heads. In contrast, the motor-pump and total efficiencies for this particular system were reported at 23% and 1.5%, respectively.

In Reference [21], an investigation into the impact of shading on the performance of Photovoltaic Pumping Systems (PVWPS) in Bejaia-Algeria is documented. The study explores ten distinct partial shading scenarios to explicitly outline the effects of shadows on the PVWPS operation. The results indicate a significant reduction of 50% in PV production when the PV array is subject to shading, resulting in a degradation of overall system efficiency. Specifically, the

efficiency drops from 1.299% (without shading) to 0.83% (with shading). Furthermore, two shading instances resulted in a system shortage, emphasizing the adverse effects of shadowing on the functionality of the PVWPS. It was concluded that it is better to have a completely shaded string than several partially shaded ones.

In Reference [22], a comparative analysis of a PVWPS with different configurations is outlined. The study encompasses four distinct systems, each featuring varied PV array setups. The first configuration (PVWPS1) is comprised of three parallel strings, with each string consisting of six 75W modules connected in series (6S×3P). The subsequent configurations (PVWPS2, PVWPS3, and PVWPS4) are characterized by setups of 12S×2P, 8S×3P, and 6S×4P, respectively. Experimental tests were conducted for these systems under sunny solar conditions and an 80m water head.

The results indicate that PVWPS3 exhibited the highest performance, supplying a maximum daily water volume of 22 m3 and achieving the highest average pumping efficiency (45.06%) compared to the other configurations. It also had the highest fill factor among the rest which contributes immensely to the efficiency of a PVWPS. Furthermore, the overall efficiency of the fourth system remained relatively constant throughout the operation period, except during periods of low sunlight. In contrast, the electric power generated by PVWPS3 was found to be the most suitable for the DC pump, ensuring optimal power operation.

I.10. Conclusion

In conclusion, photovoltaic water pumping systems represent a paradigm shift in sustainable water management, offering a viable solution to water access challenges while reducing reliance on fossil fuels. Through their efficient utilization of solar energy, these systems empower communities to harness nature's abundant resources for essential water supply needs. As we've explored the various types, functionalities, and design considerations, it's evident that photovoltaic water pumping systems hold immense potential for driving socio-economic development and environmental conservation. With ongoing advancements in technology and increasing adoption worldwide, these systems are poised to play a pivotal role in shaping a more resilient and sustainable future. By embracing innovation and collaboration, we can maximize the

benefits of photovoltaic water pumping systems, ensuring equitable access to clean water for generations to come.

CHAPTER II

POWER CONVERTERS FOR PHOTOVOLTAIC WATER PUMPING SYSTEMS

II.1. Introduction

In the field of power electronic converters, a diverse array of technologies converges to shape the landscape of modern electrical systems. These converters serve as the pivotal link between different energy sources and loads, enabling efficient and controlled transfer of power across various applications. In our project, we embark on a focused exploration of two critical components: the DC-DC booster and the inverter.

At the heart of our endeavor lies the imperative to transform a 30-volt DC input into a 220-volt AC output, a task paramount for the operation of a water pump, specifically designed for a fountain. This journey delves deep into the intricacies of converter design and control methodologies, where precision and efficacy are paramount.

Through this exploration, we not only seek to fulfill the immediate requirements of our project but also aspire to contribute to the broader discourse on power electronics. Our focus on the DC-DC booster and inverter underscores their pivotal roles in bridging the gap between DC input and AC output, facilitating the implementation of our fountain's vision.

II.2. Power converters

A power converter is a necessary electrical device in daily life that transforms electrical energy from one form to another. It encompasses a wide array of functions, including converting alternating current (AC) to direct current (DC) and vice versa, adjusting voltage or frequency levels, or combining these functions in various configurations. Power converters can range from basic transformers to intricate resonant converters, offering a diverse set of applications in power engineering and electrical systems components. [23]

Overall, power converters are essential devices in electrical engineering, enabling efficient and controlled electrical energy conversion to meet the specific needs of diverse applications across various industries and sectors. The following figure II.I shows placement of power converters in an electrical circuit.

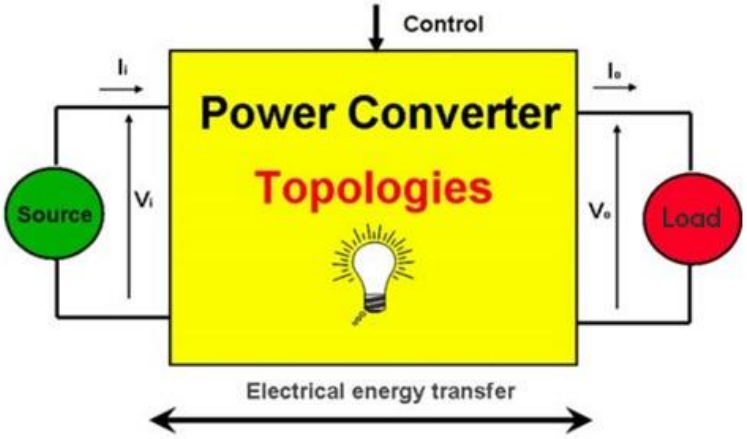

Fig. II.1. Power converter's placement in electrical circuit

A static converter is a meshed network of electrical components that acts as a linking, adapting, or transforming stage between two sources, typically between a generator and a load. It is composed of a set of electrical components, including non-linear elements like semiconductors and linear reactive elements like capacitors, inductances, and mutual inductances or transformers. These reactive components are used for intermediate energy storage, voltage and current filtering [24] [25].

II.3. Types of static converters

Static converters can be globally classified into four basic types: DC to DC, AC to AC, DC to AC and AC to DC.

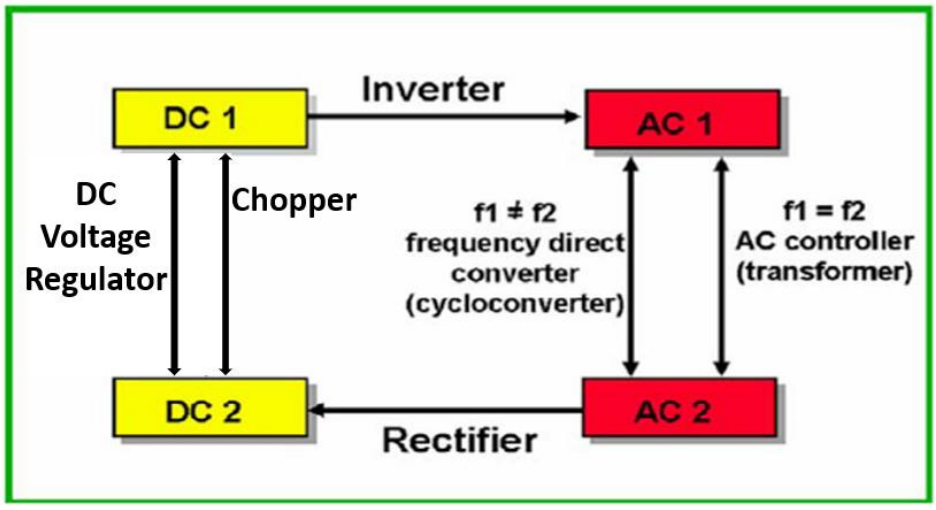

Fig II.2. Power Converter Classification

II.4. DC/DC Converters

DC/DC converters change the magnitude of direct current from one level to another. They are categorized into linear converters (Voltage regulators) and switching converters (choppers). The primary contrast lies in their operational mechanisms: linear converters maintain a continuous current flow from the input to the load to sustain the desired load voltage. They are preferred for applications requiring low power and precise regulation at the board level, or where a noise-free power source is crucial, such as in analog, audio, or interface circuits.

On the other hand, switching converters regulate the current flow by modulating the input voltage, controlling the average current through a percentage of on-time, known as the duty cycle. When the load demands higher current, the duty cycle is adjusted accordingly to accommodate the change. DC/DC converters employing switching mechanisms are widely favored in modern low and medium-power supply systems.

II.4.1. DC Voltage regulators

The effectiveness of a power supply hinges on various factors, including load voltage, load current, load regulation (LR), and other considerations. Load regulation, also known as LR or the load effect, quantifies the alteration in regulated output voltage as the load current shifts from its minimum to maximum level. Mathematically, LR is calculated by subtracting the rated full-load terminal voltage (U_{FL}) from the no-load terminal voltage (U_{NL}):

$$LR = U_{NL} - U_{FL} \quad \text{(II.1)}$$

This load regulation is commonly represented as a percentage by dividing the load regulation by the full-load voltage and then multiplying by 100 percent:

$$\%LR = (U_{NL} - U_{FL}) / U_{FL} * 100 \quad \text{(II.2)}$$

A voltage regulator, essentially, is a circuit designed to maintain a constant DC load voltage even when confronted with significant fluctuations in line voltage and load resistance. It operates as an extremely stable DC voltage source, characterized by its negligible output resistance, nearly zero.

To enhance load regulation, a controller may employ feedback from the output or feedforward from the input of the converter. This configuration aids in achieving superior regulation of power and resilience against variations in load and line conditions (fig II.3). The

primary objective of such a controller is to uphold the output at a predetermined level established by the reference. In a closed-loop control system, the measured feedback signal is compared with the desired reference, forming the fundamental structure for regulation [26].

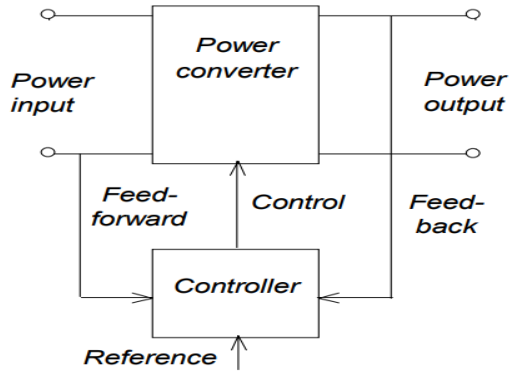

Fig II.3. Structure of a DC voltage regulator

The linear converters offer the designer four major advantages:

- Simplicity and Low Cost: Linear converters offer a straightforward and cost-effective solution.
- Quiet Operation and Load-Handling Capacity: They operate quietly and are effective at handling varying loads.
- Minimal Electrical Noise on Output: Linear converters produce little to no electrical noise on their output.
- Very Short Load Response Time: They exhibit rapid response times when the load changes.

Despite these benefits, linear regulators have certain limitations that restrict their range of applications:

- Limited to Step-Down Regulation: Linear regulators can only perform step-down regulation.
- Requirement of Off-Line Components: In off-line applications, a transformer with rectification and filtering must be placed before using linear regulators.
- Single Output per Regulator: Each linear regulator is capable of providing only one output.

- Low Efficiency: Normal applications of linear regulators yield efficiencies of only 30 to 60%, leading to significant power loss and bulkiness in high-power applications.

Because of this, linear regulators tend to get bulky at power applications.

II.4.2. Choppers

Switching supplies, such as choppers or switching DC converters, offer greater versatility compared to linear regulators, making them suitable for a broader array of applications. The primary functions of choppers or switching DC converters include:

• Voltage levels changing.

• Galvanic disconnection of electronic circuits providing.

• Output voltage stabilizing.

Choppers overcome many of the limitations of linear regulators:

- Achieving efficiencies between 65 to 90%, irrespective of output voltage, reducing the need for large heat sinks.

- Operating at high frequencies, resulting in smaller magnetic and capacitive elements for energy storage, making switching supplies more cost-effective compared to linear regulators.

- Enabling the output voltage to vary above and below the input voltage level.

- By converting input voltage into an AC waveform and utilizing magnetic elements, choppers can provide multiple output voltages, enhancing their versatility.

The drawbacks of switching converters are relatively insignificant:

- Increased complexity
- Significant generation of noise on both their output and input, which is emitted into the environment
- Considerable delay in their transient response time when reacting to load changes due to the time-limited pulses of energy

The fundamental topologies of converters are step-down and step-up. The fundamental modes of operation that form the basis of all choppers are forward-mode operation (buck) and fly back-mode operation (boost). Both modes consist of four functional components namely; a power switch, a rectifier (catch diode), an inductor, a capacitor. Therefore, in this project our focus is on step up choppers in particular boost converters [27].

II.5. DC-DC Boost converter

Step-up converters typically produce output voltages higher than the input voltage. However, by modifying the chopper commutation, higher load voltages can be achieved.

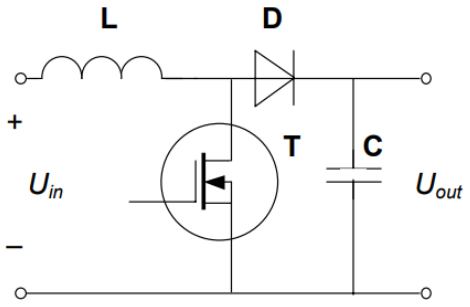

Fig II.4. A simple circuit of the DC-DC booster

- The fly-back operation can be divided into two periods:

1. Switch-On Period: When the power switch is on, current flows through the inductor, storing energy within its coil material. The inductor current increases almost linearly during this phase.

2. Switch-Off Period: Once the switch turns off, the inductor current cannot change instantaneously, forcing it to flow through the diode and the load. As a result, the inductor's voltage reverses (flies back), causing the diode to turn on and transfer the inductor's energy into the capacitor. Consequently, the inductor current decreases. This cycle repeats until the energy of the inductor is depleted.

Since the inductor voltage flies back above the input voltage, the voltage of the capacitor becomes higher than the input voltage. When the capacitor voltage reaches the desired level, the switch turns on again. As the capacitor cannot discharge via the switch (due to the reverse-biased diode), a stable voltage typically twice the U_{IN} or more can be obtained.

Mathematically, the output voltage can be expressed as:

$$Ve = (1-\alpha) * Vs \quad (II.3)$$

Where (α) represents the duty cycle, and for a variation of α in the range ($0 < \alpha < 1$), the output voltage varies in the range ($V_e < Vs < +\infty$). This circuit is particularly advantageous when operating on low-voltage supplies and can lead to very cost-effective converter designs [28].

II.5.1 Modeling of a DC-DC booster

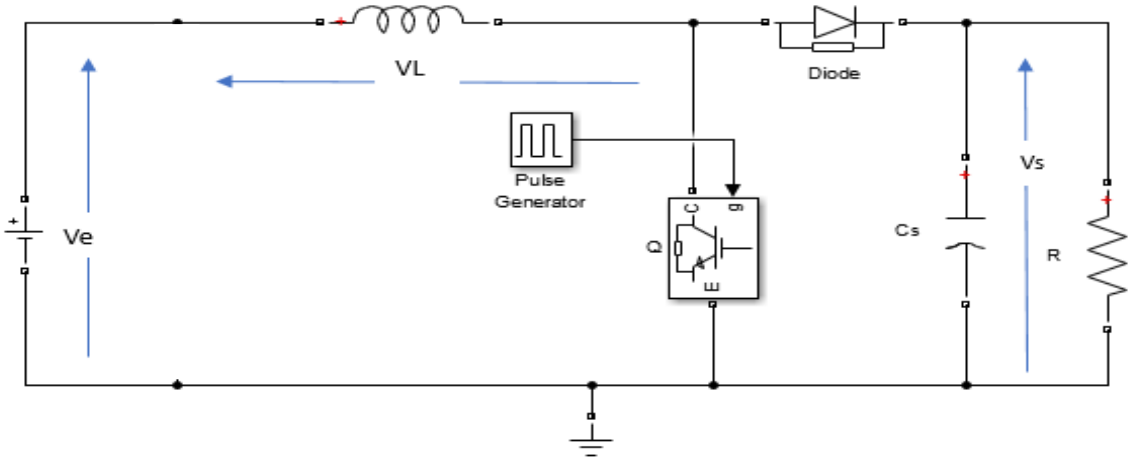

Fig II.5. A detailed circuit of DC-DC booster in MATLAB

- **First interval: 0< t<αT**

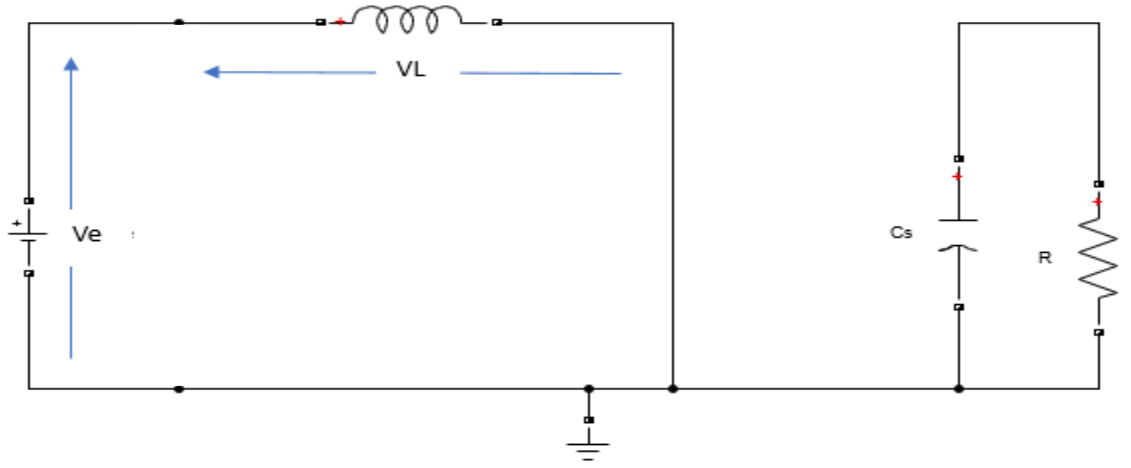

Fig II.6. The first interval circuit (charge)

From the Kirchoff's voltage law we have: $Ve - V_L = 0$

$$So \quad V_e = L \frac{d I_L(t)}{dt} \text{ è } I_L(t) = \frac{Ve}{L} \int_0^t dt = \frac{Ve}{L} t + Cste$$

Introducing limits,

$$I_L(0) = 0 + Cste = Cste = I_{Lmin} \tag{II.4}$$

$$I_L(\alpha T) = \frac{Ve}{L} \alpha T + I_{Lmin} = I_{Lmax} \tag{II.5}$$

We then have $\Delta I_L = I_{Lmax} - I_{Lmin} = \frac{Ve}{L} \alpha T + I_{Lmin} - I_{Lmin}$

Therefore $\Delta I_L = \frac{Ve}{L} \alpha T$ (II.6)

- **Second interval: αT<t<T**

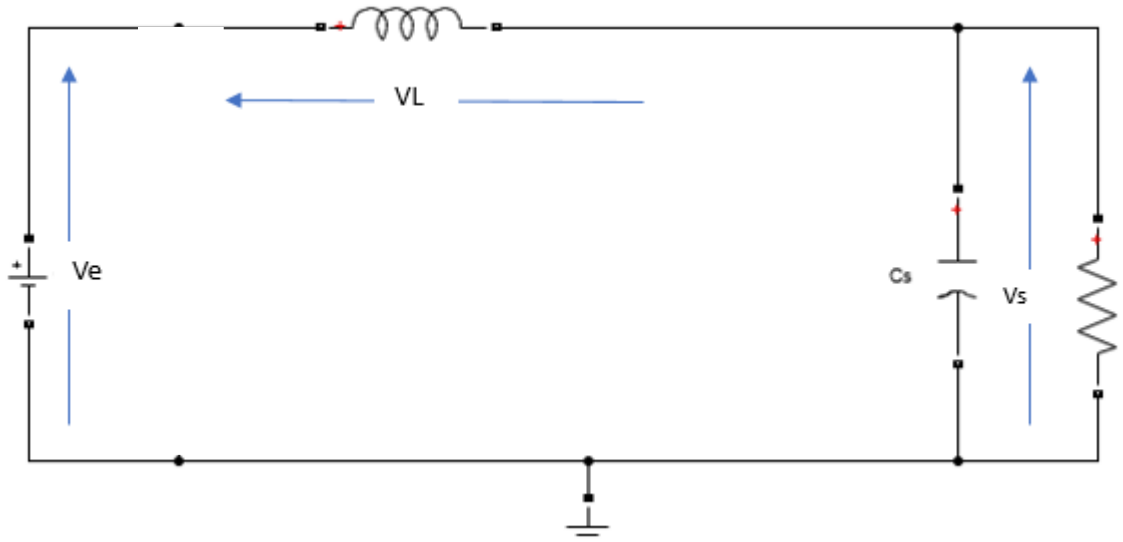

Fig II.7. The second interval circuit (discharge)

Therefore, from Kirchoff's voltage law we have: $V_e - V_L - V_s = 0$

So $V_e - V_s = L \frac{dI_L(t)}{dt}$ è $I_L(t) = \frac{V_e - V_s}{L} \int_{\alpha T}^t dt = \frac{V_e - V_s}{L} (t - \alpha T) + Cste$

Introducing limits,

$$I_L(\alpha T) = 0 + Cste = Cste = I_{Lmax} \quad (II.7)$$

$$I_L(T) = \frac{V_e - V_s}{L}(T-\alpha T) + I_{Lmax} = I_{Lmin} \quad (II.8)$$

Therefore $\Delta I_L = I_{Lmax} - I_{Lmin} = I_{Lmax} - I_{Lmax} + \frac{V_s - V_e}{L}(T-\alpha T)$

$$\Delta I_L = \frac{V_s - V_e}{L}(T-\alpha T) \quad (II.9)$$

❖ Now to get the relation between the input voltage and the output voltage, (II.5) = (II.8)

$$V_s = \frac{V_e}{(1-\alpha)} \quad (II.10)$$

- Ideally in all statics power converters, there is no loss in power

So $P_e = P_s = P$

Then $V I = V_e I_e = V_s I_s$ è $\frac{V_e}{v_s} = \frac{I_s}{I_e}$

Therefore $I_e = \frac{I_s}{1-\alpha}$ (II.11)

In most cases, the filtering inductor value L is selected to keep the current ripple below a certain limit I_{Lmax}. Thus, the inductor value can be calculated as

$$L_{min} = \frac{Ve}{\Delta I_L . f}(\alpha)^2 \quad (II.12)$$

In the boost converter, the current is delivered to the output RC circuit only when diode α is conducting. Thus, this current is discontinuous which implies a large filter capacitor requirement to limit the output voltage ripple. The filter capacitor must provide the output dc current to the load when the diode α is not conducting. The minimum value of the filter capacitance that results in the voltage ripple ΔVs is given by; [25]

$$C_{min} = \frac{Ve}{\Delta V_s .8.L . f^2}(\alpha)^2 \quad (II.13)$$

II.6. Boost regulators

The described circuit is a step-up or boost regulator, depicted in Figure II.8a, which operates similarly to a fly-back regulator but includes feedback. This configuration enables the

output voltage to exceed the input supply voltage. Such regulators find applications in power supplies, active filters, and reactive power compensators [29].

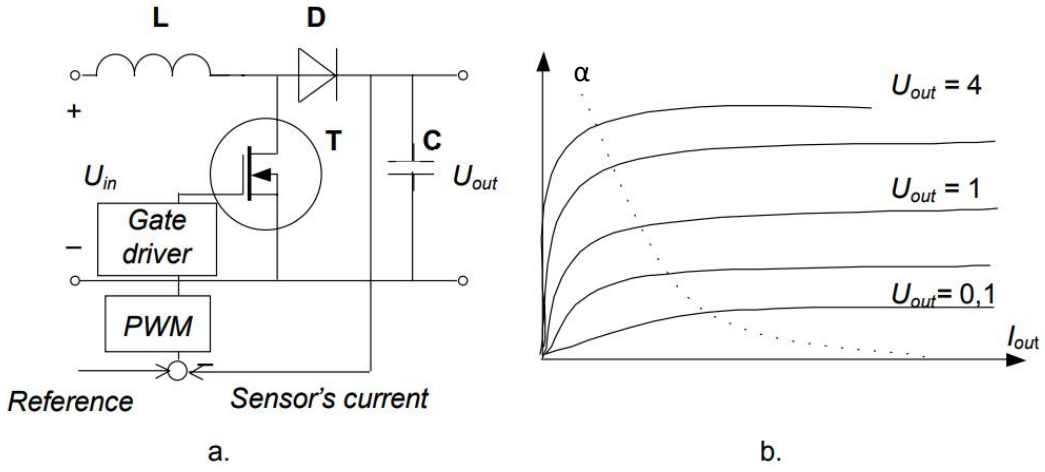

Fig II.8. Boost regulator circuit

The output voltage depends on the relative duty cycle of the switch, as depicted in Figure II.8b. However, it's important to note that the boost regulator may have poor ability to prevent hazardous transients or failures within the supply. To address this, transformer isolation is used to significantly enhance the regulator's performance and safety.

In a nutshell, a DC/DC converter tasked with generating a voltage higher than the supply voltage needs to store energy in the input reactive element (usually an inductor) and subsequently transfer it to the output reactive element (typically a capacitor), but at different time intervals. This control over the energy transfer is achieved by adjusting the duty cycle, either with or without feedback mechanisms.

II.7. Inverters

Inversion is the process of converting DC voltage into AC voltage, performed by a device called an inverter. It utilizes semiconductor devices like transistors and thyristors such as SCR and GTO to regulate the frequency of the AC output voltage. The DC input voltage can come from a rectified output of an AC power supply or an independent source like a battery. The inverter's output frequency is adjustable by controlling the switching frequency of its devices, typically

through a clock oscillator. However, achieving pure sinusoidal waveforms is complex and costly due to the presence of harmonic content in the AC output. [27]

Therefore, there are two methods used to reduce harmonic content:

- Utilizing a filter circuit on the inverter's output, though it must manage high power output.

- Employing a modulation strategy to alter the output voltage's harmonic content, potentially minimizing or eliminating the need for filtering depending on the amplification type.

• Inverters can be classified depending on the various ways as follows:

II.7.1. Classification as per the way of input source

In power electronics, inverters are classified as current source inverters (CSIs) and voltage source inverters (VSIs). CSIs generate a constant current output by controlling the input current, making them suitable for applications requiring a stable current. VSIs generate a stable voltage output by controlling the input voltage, and are widely used where a stable voltage supply is essential. Both types are crucial in different applications, offering unique advantages based on specific system requirements.

Voltage source inverters generate voltage with specific characteristics like magnitude, frequency, and phase. VSIs are widely used due to their versatility, providing a stable output similar to a voltage source, featuring low internal impedance and utilizing capacitors for voltage stability, while both types of inverters are crucial, voltage source inverters (VSIs) offer particular advantages due to their stable voltage output and low internal impedance, making them suitable for applications where maintaining voltage stability is crucial, such as in renewable energy systems or motor drives [29].

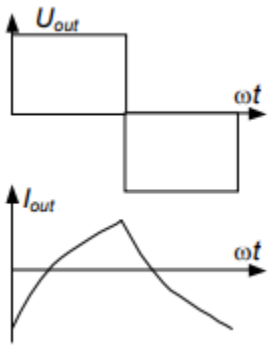

Fig II.9. Output current and voltage in voltage source

Another aspect to consider is that the switches must be created using fully controllable devices such as transistors, thyristors, GTOs or MCTs along with free diodes. The output current of VSI is modulated based on both the voltage value and the load resistance. However, there are options to adjust the output voltage of the inverter. One common method involves changing the DC input voltage provided to the inverter, which subsequently affects the output voltage. This modification occurs externally to the inverter and acts independently of its function. Alternatively, the inverter can internally modulate the AC voltage to achieve voltage variation.

II.7.2. Classification as per the waveform of the output voltage

Inverters can be classified by their output voltage waveform into three main types: square-wave, modified sine wave, and pure sine wave inverters. Modified sine wave inverters produce a waveform that approximates a square wave with some smoothing, reducing distortion. Pure sine wave inverters deliver a smooth, continuous sine wave similar to utility power, essential for sensitive electronics.

Square-wave inverters generate a simple alternating waveform with two fixed levels, +V and -V, making them cost-effective but prone to high harmonic distortion. While economical and straightforward, square-wave inverters generate high harmonic content and are less suitable for sensitive applications, making them ideal only for basic uses where cost is a primary concern [29].

II.7.3. Classification as per the association

Inverters can be categorized by their association with the power grid into two main types: offline inverters and online inverters. Online inverters, or grid-connected inverters, synchronize their output with the grid's voltage and frequency, making them suitable for grid-tied solar power systems where excess energy can be fed back into the grid.

Standalone inverters, also known as autonomous inverters, operate independently of the grid, generating AC power directly from DC sources like batteries or solar panels. They are commonly used in standalone systems such as off-grid solar power setups or uninterruptible power supplies (UPS). Offline inverters are essential for providing reliable power in locations without grid access, ensuring energy independence and continuous power availability [30].

II.7.4. Classification as per its phases

Inverters can be classified based on their internal design into three main types: single-phase, three-phase, and multilevel inverters. Three-phase inverters convert DC power into three-phase AC power using six switches arranged in a bridge configuration. They are crucial for industrial and commercial applications requiring three-phase power, like motor drives and grid-tied inverters for electrical distribution. Multilevel inverters, comprising two or more distinct voltage levels, offer a stepped approximation of a sine wave by utilizing multiple voltage levels. This approach provides several advantages over traditional two-level inverters, which produce a basic square wave output.

Single-phase inverters, on the other hand, are power electronic devices that convert DC power into single-phase AC power using a pair of switches. They are commonly utilized in small-scale applications such as residential solar photovoltaic systems or small wind turbines, providing a straightforward solution for converting DC power into single-phase AC power [29].

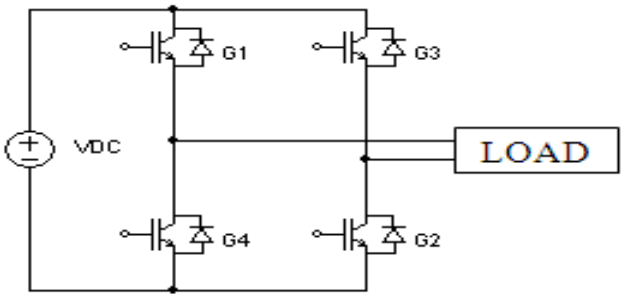

Fig II.10. A single-phase inverter circuit

II.7.5. Classification based on Internal Design

Inverters can also be classified based on their internal design into different configurations, such as half-bridge and full-bridge inverters. A half-bridge inverter utilizes two switches connected in series with the load, forming a simpler and more cost-effective design suitable for low to

medium power applications. Its basic operation involves switching the two switches alternately to generate an AC output waveform. While effective for certain applications, it may not provide bi-directional current flow.

In contrast, a full-bridge inverter employs four switches arranged in a bridge configuration, allowing for bi-directional current flow. This complexity makes it suitable for high-power applications or those requiring features like regenerative braking, as seen in electric vehicles. The full-bridge configuration provides advantages over half-bridge inverters, such as increased power handling capability and flexibility in current flow direction [29].

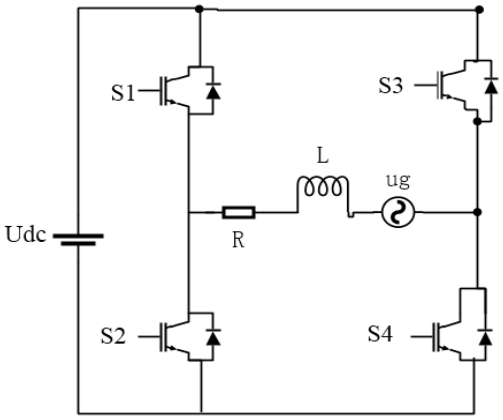

Fig II.11. A full bridge inverter circuit

II.8. Mode of operation of a full-bridge inverter

Different techniques for controlling electrical inverters can be classified in various ways namely symmetrical control (block control), asymmetrical control and Pulse Width Modulation (PWM).

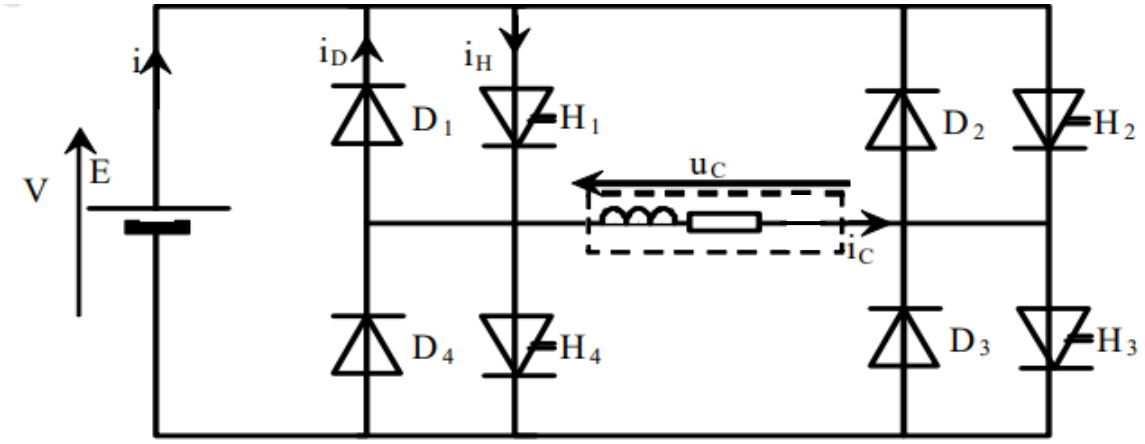

Fig II.12. Structure of a single-phase inverter

II.8.1. Symmetrical control

This command consists of controlling the switches of a single-phase inverter H1 and H3 on closing for a half-period then controlling H2 and H4 during the second half-period. So, each switch is closed for half the period. The states of switches H1 and H4, H2 and H3 must be complementary to avoid short-circuiting the voltage source.

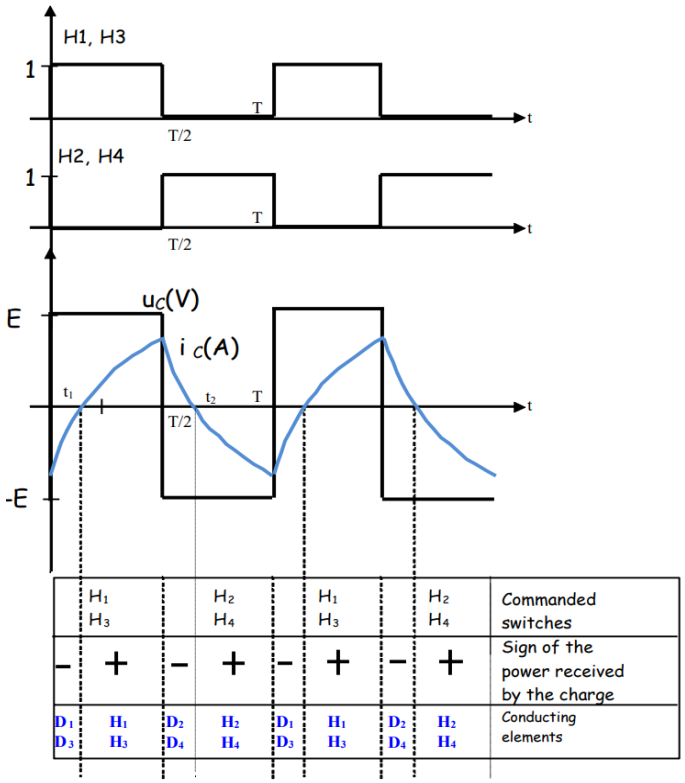

Fig II.13. Output waveforms for symmetrical control

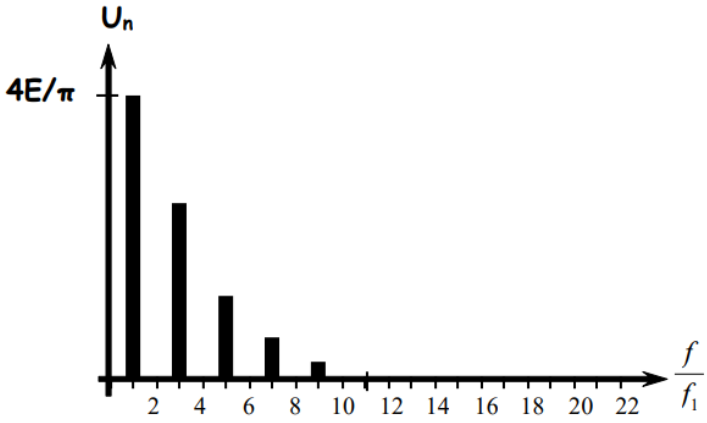

Fig II.14. Output voltage spectrum for symmetrical control

The voltage spectrum in fig II.14 shows that with symmetrical control, the output voltage is rich in harmonics (ripples). Indeed, the voltage uc(t) is an odd slot function, its decomposition only contains sine terms and only presents odd harmonics:

$$u_c = \sum_{k=0}^{\infty} \frac{4E}{(2k+1)\pi} sin\,(2k+1)\omega t \quad \text{(II.14)}$$

* This type of command is the simplest to implement. On the other hand, the output voltage is very rich in low order harmonics (low frequency) which makes filtering difficult.

* Since the current is not sinusoidal, it is rich in harmonics (of the same frequencies as the tension).

* Full-wave control (block/symmetrical control) imposes a fixed RMS (root mean square) value on the load (U_C= E). Its adjustment is possible only by adjusting the voltage E (through a chopper, controlled rectifier)

II.8.2. Asymmetrical control

Also known as shift control, this command allows you to modify the characteristics of the output voltage, in particular the RMS value of its fundamental, without having to intervene at the level of the supply voltage E. The command intervals remain equal to half a period but are shifted as shown below in figure II.15.

To do this, we simply shift the switch control by an angle t (shift angle).

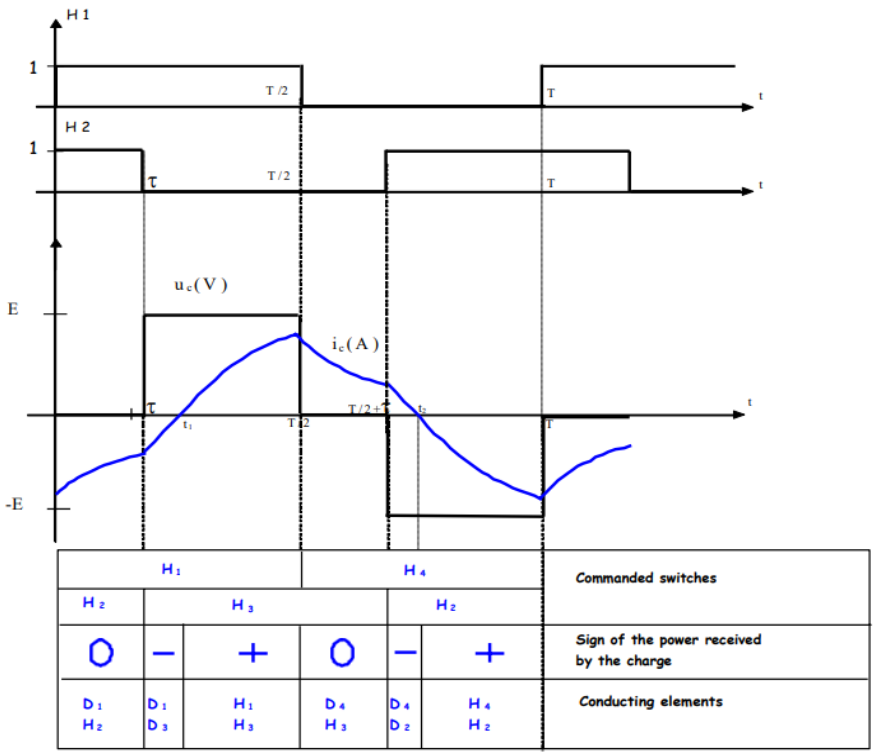

Fig II.15. Output waveforms for asymmetrical control

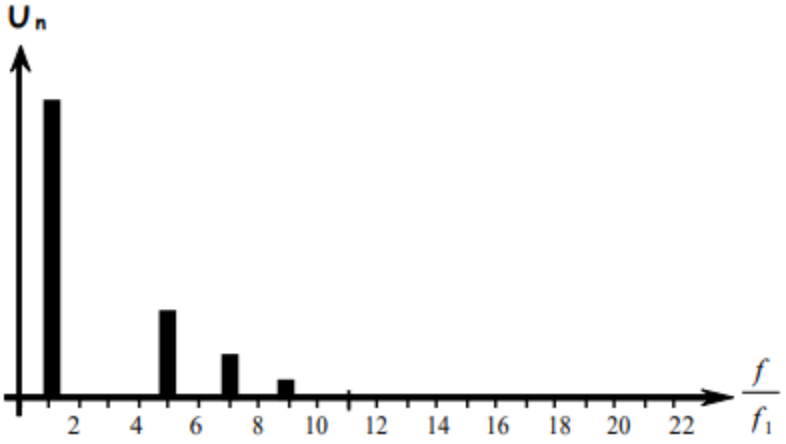

Fig II.16. Output voltage spectrum for asymmetrical control

Observation of the spectrum shows that the shift control inverter presents a more favorable spectrum than that with symmetrical control. Indeed, the Fourier series decomposition of the output voltage is written:

$$v(t) = \frac{4E}{\pi} \times \sum_{k=0}^{\infty} \left[\frac{1}{2k+1} cos\big((2k+1).\beta\big).sin\left((2k+1).\omega t\right)\right. \quad \text{(II.15)}$$

Where: β = τ

We see that we can eliminate certain harmonics by a judicious choice of β. To do this, it is enough to choose the value of β which cancels the chosen harmonic k, which is verified by;

$cos\ ((2k + 1)\ \beta) = 0$

Example: to eliminate harmonic 3: k =1, so cos3β =0 which is verified by 3β=π/2. Therefore, we get β=π/6

- The root mean square (RMS) voltage:

If we plot u^2 (t), we get;

$$U^2 = \frac{E^2(\frac{T}{2}-\tau)}{\frac{T}{2}} \qquad \text{which gives:} \qquad U = E\sqrt{1 - \frac{2\tau}{T}} \tag{II.16}$$

By varying τ we can vary the RMS value of the voltage supplied by the inverter.

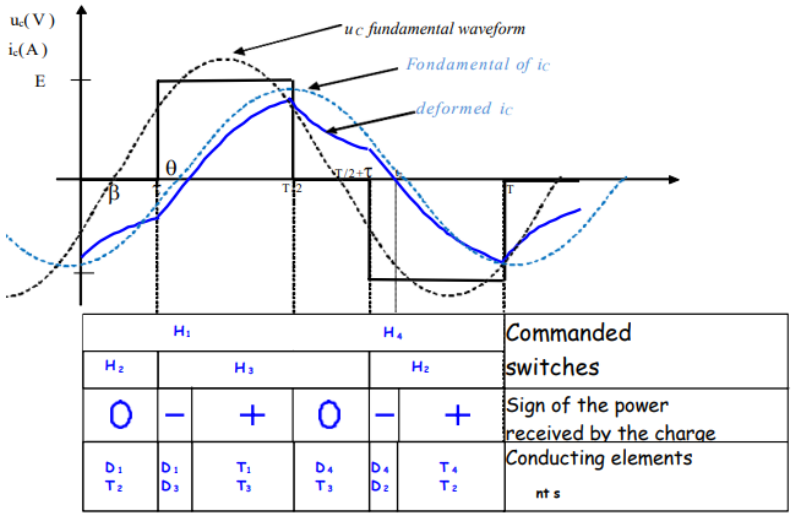

Fig II.17. The charge current

The mean value of the current is:

$$\langle i \rangle = \frac{I\sqrt{2}}{\pi}(\cos(\tau) - \cos(\theta-\tau)) \tag{II.17}$$

The power provided by the source is:

$$P = E\langle i \rangle = \frac{EI\sqrt{2}}{\pi}(\cos(\tau) - \cos(\theta-\tau)) \tag{II.18}$$

Note: the two types of command that we have seen so far have a common character: each semiconductor branch is only activated once per period (period of the output voltage = that of the commanding branch). For this, we sometimes call these methods fundamental pulsation control.

II.8.3. The Pulse Width Modulation (PWM) technique

The main purpose of this technique is to adjust the frequency and RMS value of the output voltage and to push unwanted harmonics towards high frequencies, their amplitudes then becoming negligible. This control is more complex, it is a symmetrical command presenting a large number of switching by period with openings and closings of switches of modulated durations (variable widths).

Its principle is based on obtaining the switching times of the switches by comparing two signals:

- a triangular signal Vt of high frequency fp (switching frequency)

- a sinusoidal reference signal Vref of variable amplitude and frequency f1.

These two signals are compared. The result of the comparison is used to control the opening and closing of the switches.

If Vref>Vt, α =1; If Vref<Vt, α =0

Therefore: (H1 and H3) are controlled by the signal α and (H2 and H4) are controlled by the inverse of the signal α.

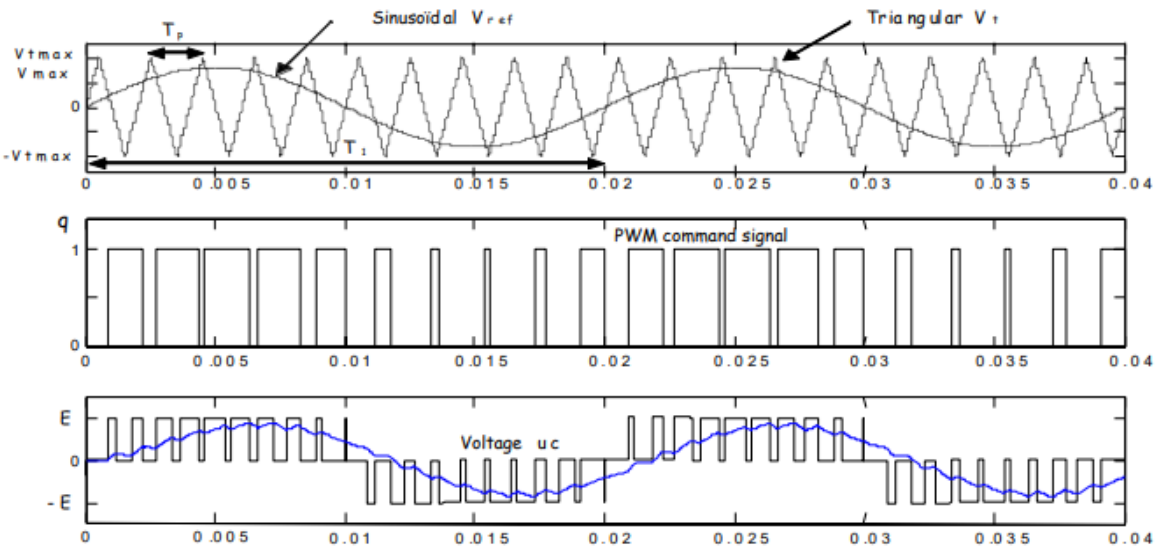

Fig II.18. PWM signal generation

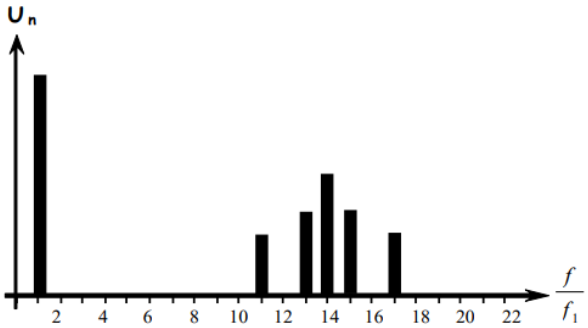

Fig II.19. Spectrum of the output voltage

Spectrum analysis shows that PWM control pushes harmonics towards high frequencies (around the switching frequency fp) which facilitates filtering of the output voltage. This command, which makes it possible to obtain a fundamental variable in amplitude and frequency, is very much used in drives for asynchronous machines.

II.9. Conclusion

As we conclude our exploration into the field of power electronic converters, we emerge with a deeper understanding of their intricacies and functionalities. Through meticulous examination, we have dissected the DC-DC booster, elucidating its various types, modeling techniques and the intricacies of control utilizing advanced microcontrollers and switching methodologies. Similarly, our journey led us to unravel the complexities of inverters, unveiling

their diverse typologies, modeling intricacies, and the art of control through Pulse Width Modulation (PWM). In this voyage of discovery, we have not only acquired theoretical knowledge but also gained practical insights into the real-world application of these converters, particularly in our quest to power a fountain pump. As we draw the curtains on this chapter, we stand poised at the threshold of implementation, armed with the knowledge and tools to engineer solutions that transcend mere functionality. Our journey continues, fueled by the promise of innovation and the relentless pursuit of excellence in the field of power electronics.

CHAPTER III

DESIGN AND IMPLEMENTATION OF THE PVWPS

III.1 Introduction

In this chapter, we present a comprehensive overview of our photovoltaic water pumping system (PVWPS). We will delve into the core components, including the DC-DC boost converter, power supply electronic card, along with the control card that orchestrates the booster's operation. This chapter will detail the design and implementation of the electronic card we developed, highlighting its integration into the overall system. Additionally, we will explore the system elements such as solar panels, MPPT controller, batteries, conversion systems, and the load, demonstrating how each component contributes to the efficient functioning of our PVWPS. By examining these elements, we aim to provide a clear understanding of the system's architecture and its operational dynamics.

III.2 System layout and description

Our Photovoltaic Water Pumping System seamlessly integrates a set of batteries and a DC-DC boost converter, leveraging a 30V output from the PV panels, we efficiently transform it into different values of amplified DC voltage. This voltage powers our motor pump, ensuring smooth and sustainable fountain operation, all powered by solar energy.

Below is figure III.1 showing the system architecture, figure III.2 showing a picture of the project site and figure III.2 showing a picture of the project site.

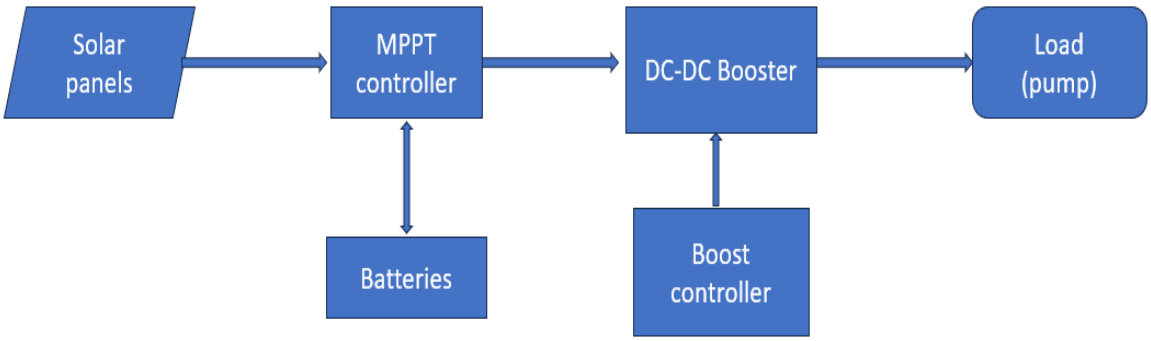

Fig III.1. System architecture

Fig III.2. A picture of the project site

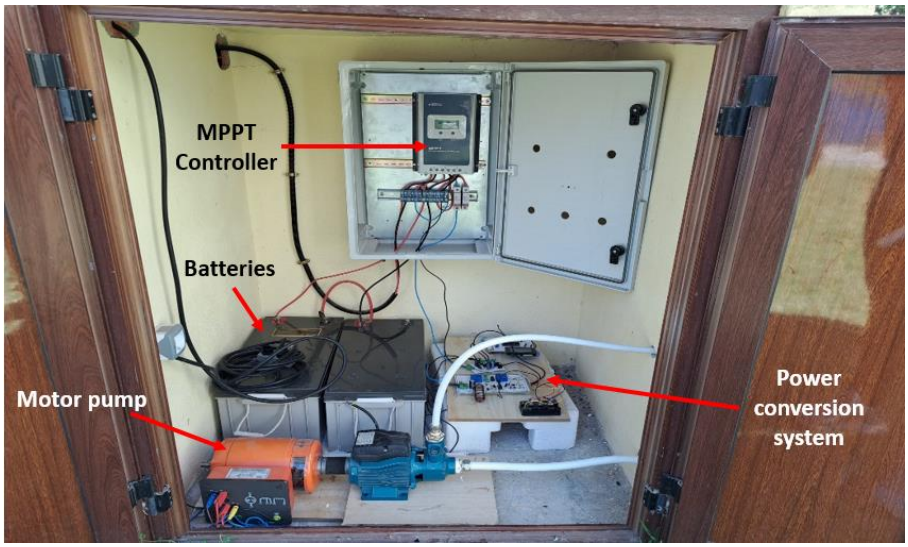

Fig III.3. A picture of the interior of the electrical cabinet

III.3 Design and implementation of the electronic cards

To generate the variable DC voltage that we need to run our fountain, we designed a set of electronic cards to facilitate our objective. These included a power supply, a DC-DC booster and its control circuit card. We designed these cards using a professional software called Altium Designer. Altium Designer is a PCB and electronic design automation software package for printed circuit boards. It allows engineers to design and customize their own circuit boards.

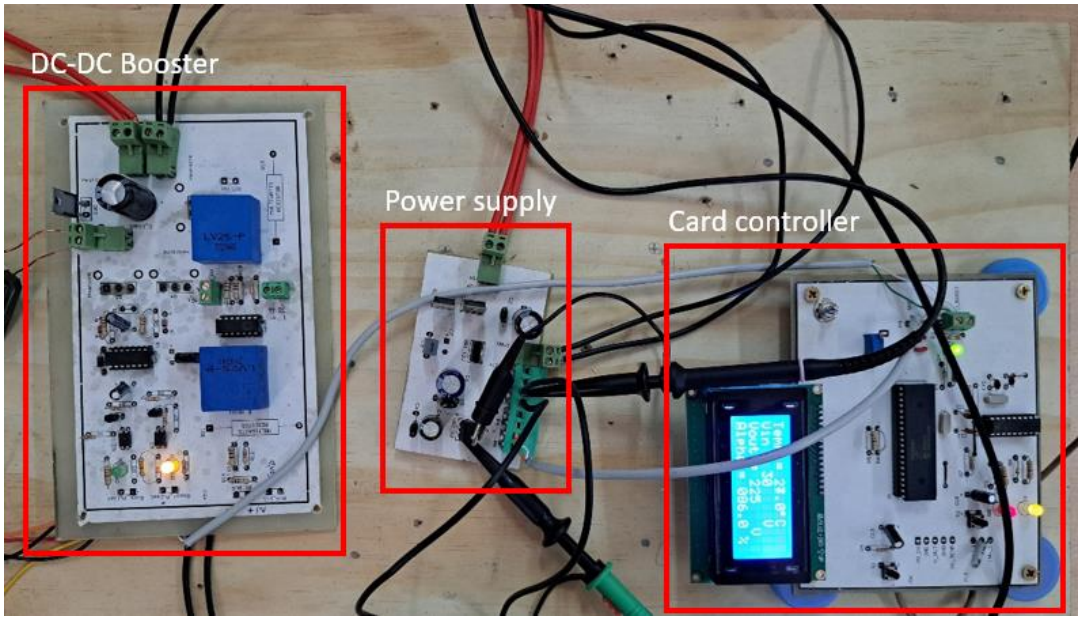

Fig III.4. A photo of all the electronic cards

III.4. The design and implementation of the power supply

This electronic card includes capacitors for filtering the different level of voltages. It also comprises of voltage regulators namely; 7815, 7805 which output 15V and 5V respectively. Their datasheets are shown in figure A4 and A5 of the appendix. From the 30V battery supply, this whole setup generates a power supply for the microcontroller of 5V and the boost converter of 15V. Below is the schematic diagram of the power supply card in Altium Designer.

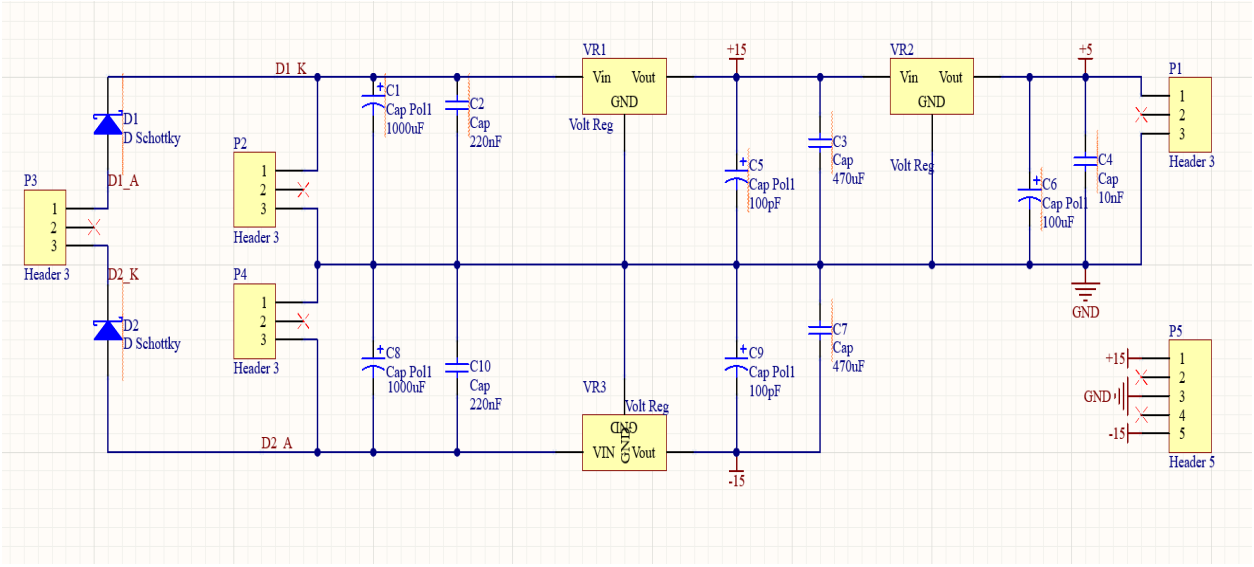

Fig III.5. Schematic diagram of the power supply card in Altium Designer

After constructing the circuit, we simulated it in Proteus 8 professional software and we obtained the following results from the oscilloscope for the 15V output and 5V output. Each division vertically represents 5V.

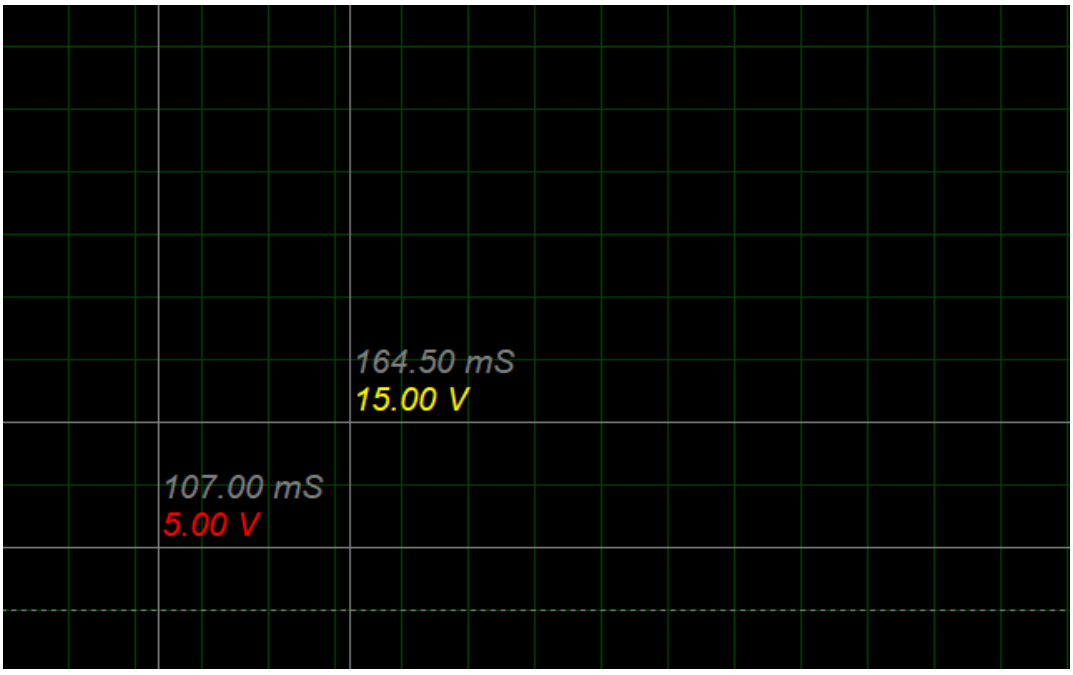

Fig III.6. Output values for the power supply circuit simulation

From there, we continued to design the PCB of the power supply in Altium Designer and it is depicted in the figure III.7a & b below.

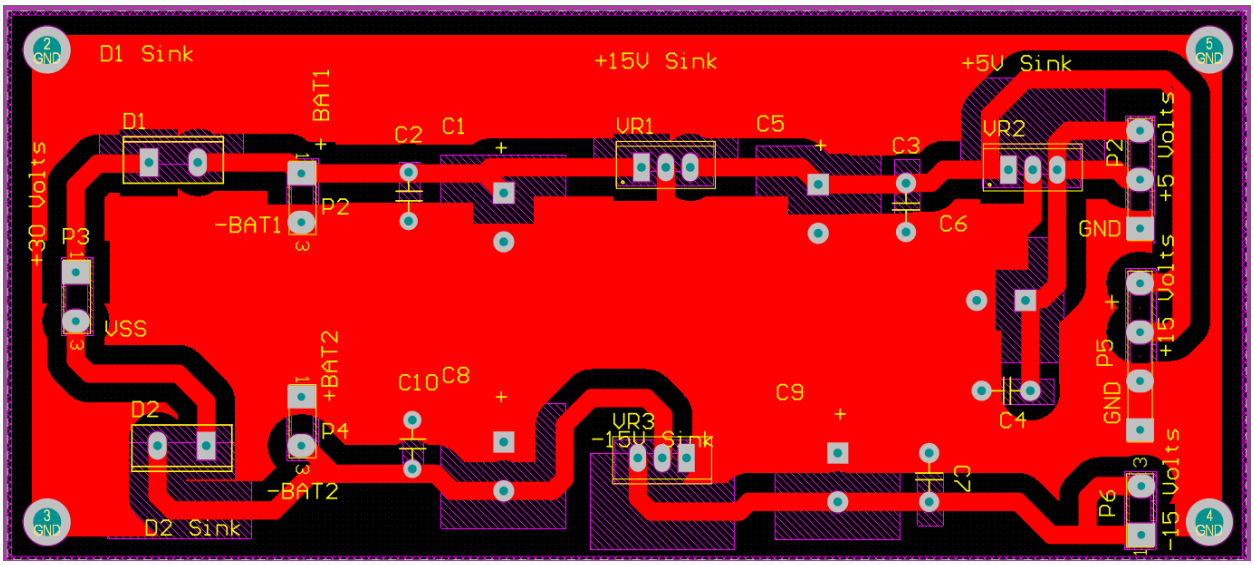

Fig.III.7a. The 2D layout of the power supply PCB

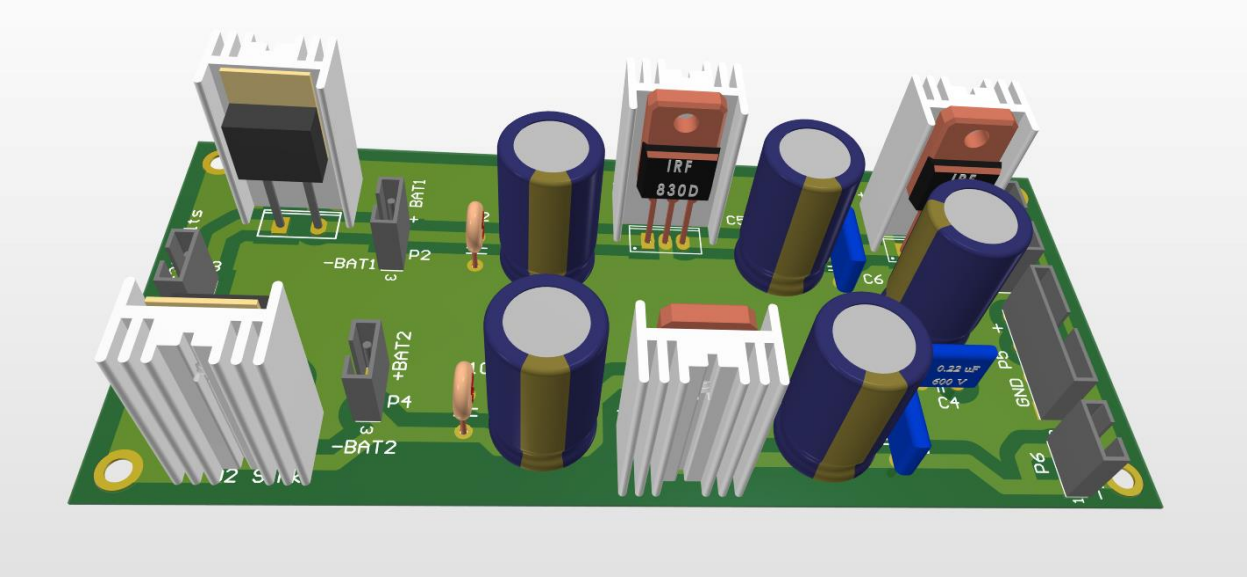

Fig.III.7b. The 3D layout of the power supply PCB

After printing out the circuit board and mounting the necessary components, the power supply electronic card is depicted in fig III.8 below.

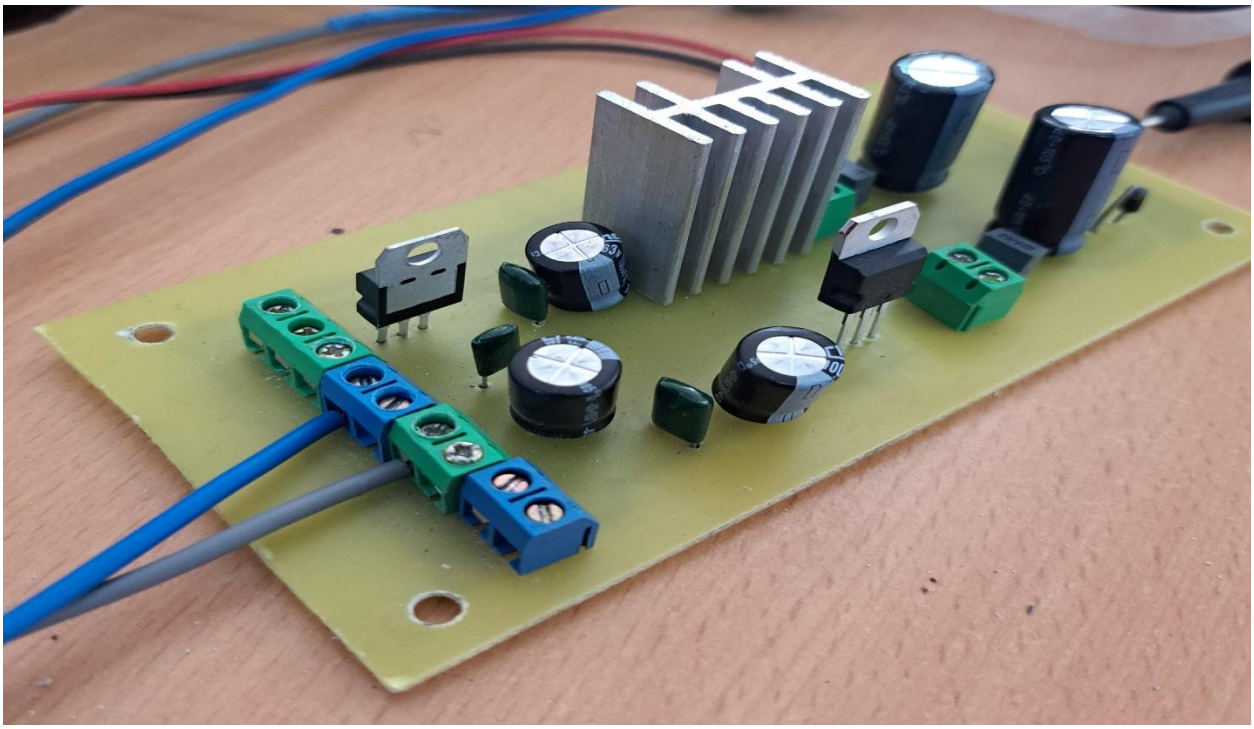

Fig III.8. The printed circuit board of the power supply

We ran laboratory tests on our power supply electronic card for verification and it successfully provided +15V and +5V which we used in our system. The figure III.9 below shows our results. The yellow channel represents the 15V graph and each vertical division is 5V. The blue channel represents the 5V graph and each vertical division is 2V.

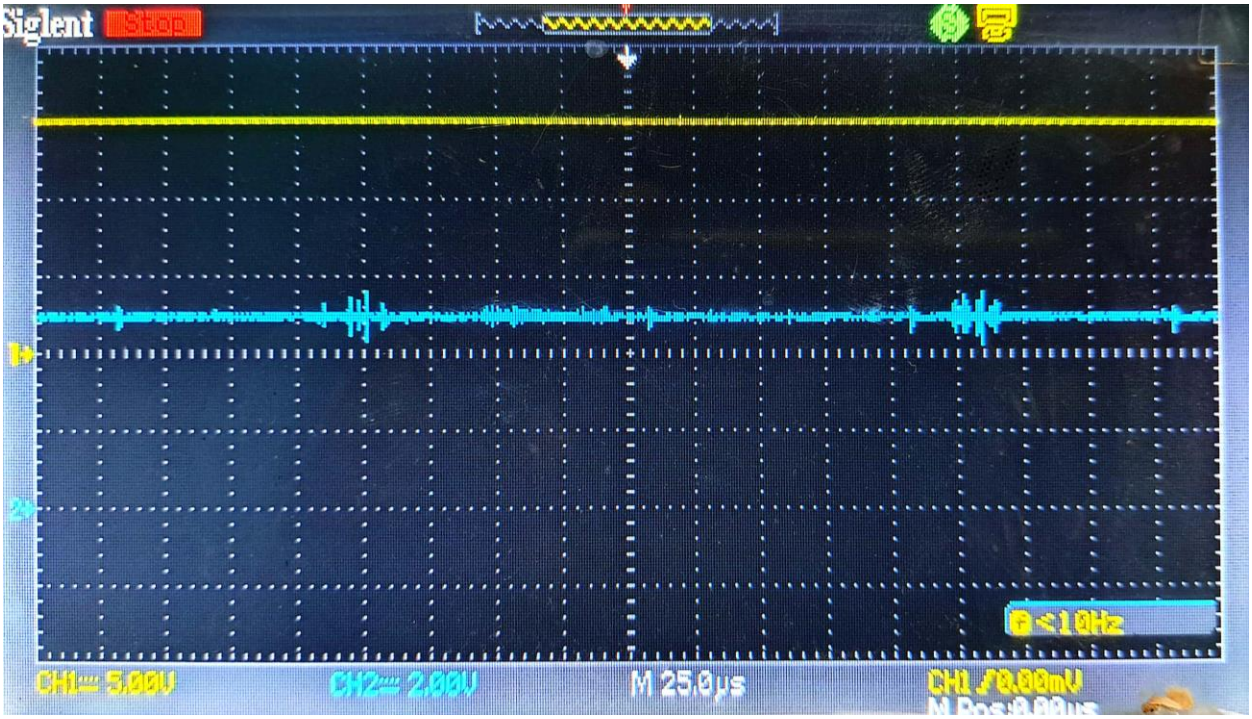

Fig III.9. The output voltage waveforms of the power supply

III.5. Design and implementation the DC-DC booster converter

In suite of our goal to obtain sustainable voltage values to power the motor-pump set, we meticulously designed and constructed the DC-DC boost converter, which had for parts, an electronic control card and the booster electronic card itself.

III.5.1. Design and implementation the booster card controller

To control the DC-DC boost, we used a PIC16F887 microcontroller to generate three duty cycles using the input and output values of the booster. With our input being 30V, we used three duty cycles of 80%, 83% and 86% to get a varying DC output of 150V, 180V and 230V so as to have different water heads for out fountain pump. We used the MicroC software to program the microcontroller. We chose the PIC16F887 microcontroller for its abundant I/O ports, integrated analog features, and PWM capabilities, ensuring precise control and efficient operation of the

boost converter coupled with its ready availability. The datasheet of the microcontroller is in figure A11 of the appendix. Below is the schematic diagram of the booster control card in Altium Designer (fig III.10). We also included a control section for an inverter, which we aim to construct as part of the future prospects of this project.

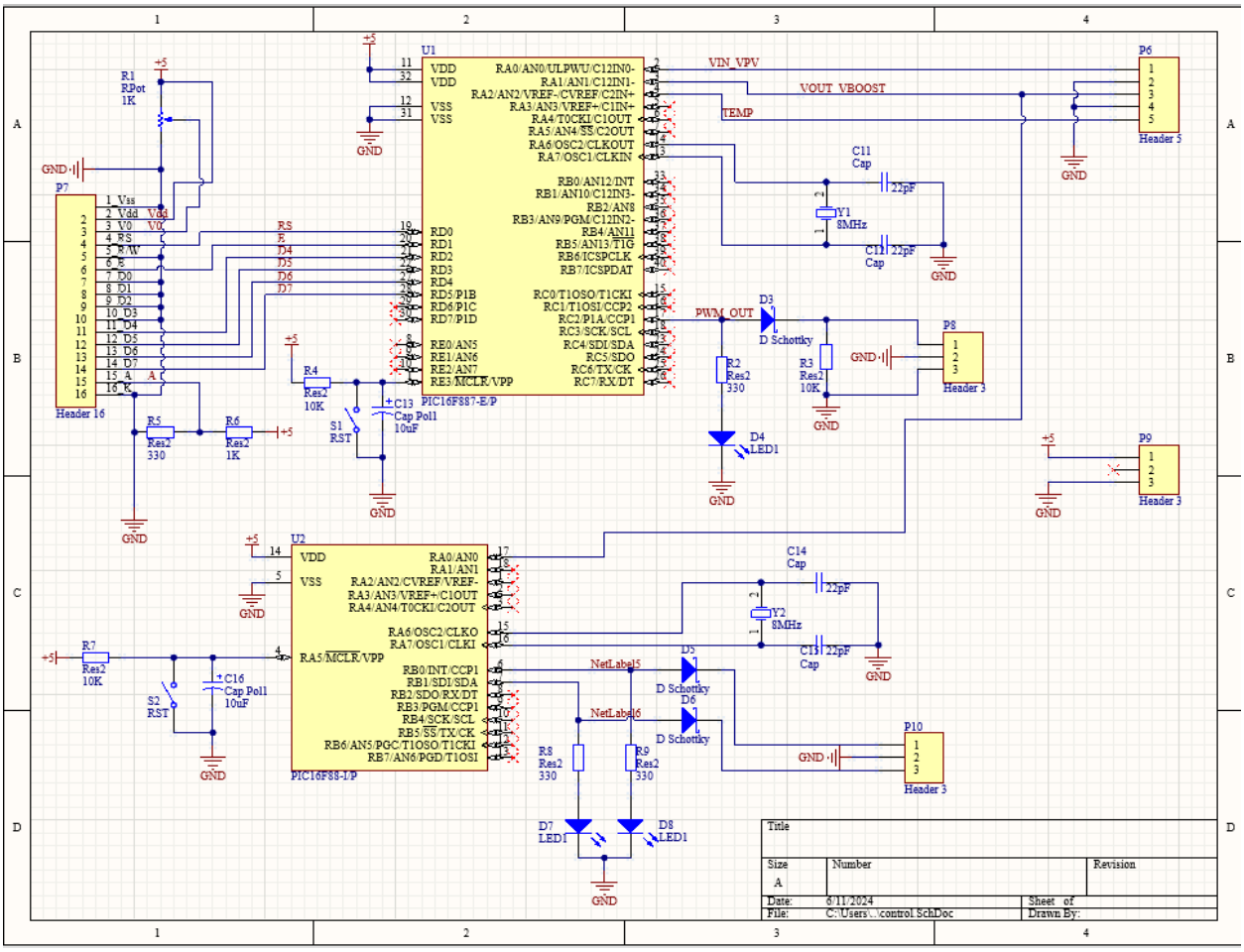

Fig III.10. Schematic diagram of the booster control card

We then simulated the above schematic in Proteus-8 Professional and obtained the following output duty cycle (α) signals indicated in following fig III.11.

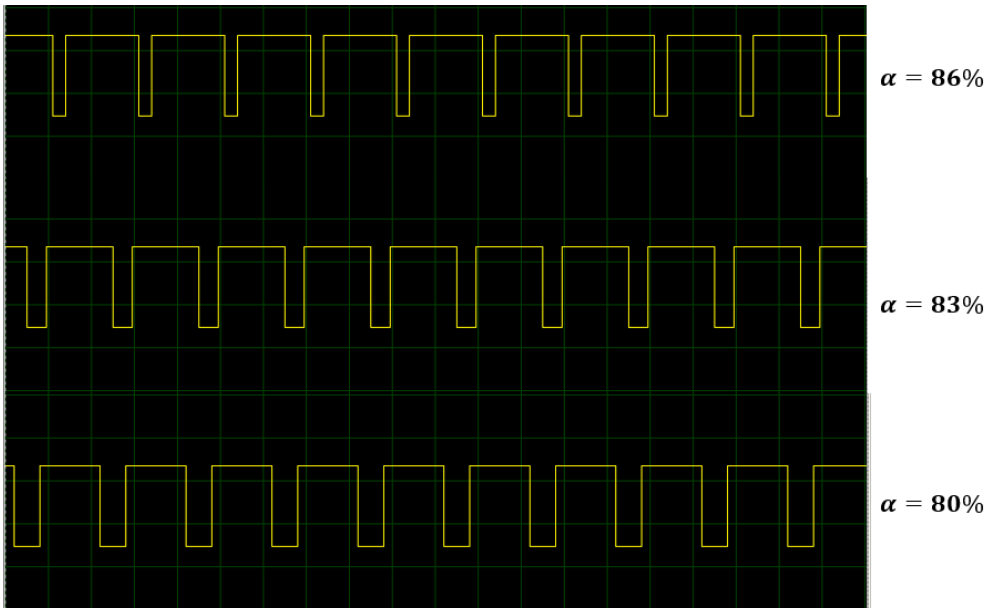

Fig III.11. Simulated output signals of the boost controller

Then next we generated and designed the PCB from the above schematic and it's depicted in figure III.12a and b below.

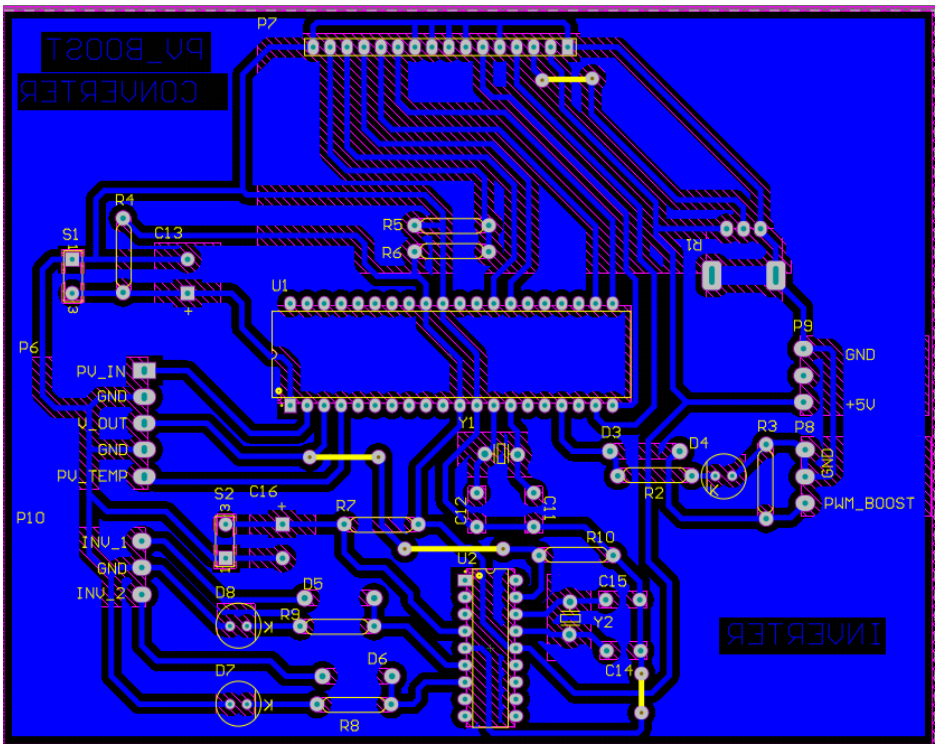

Fig.III.12a. The 2D layout of the Booster controller PCB

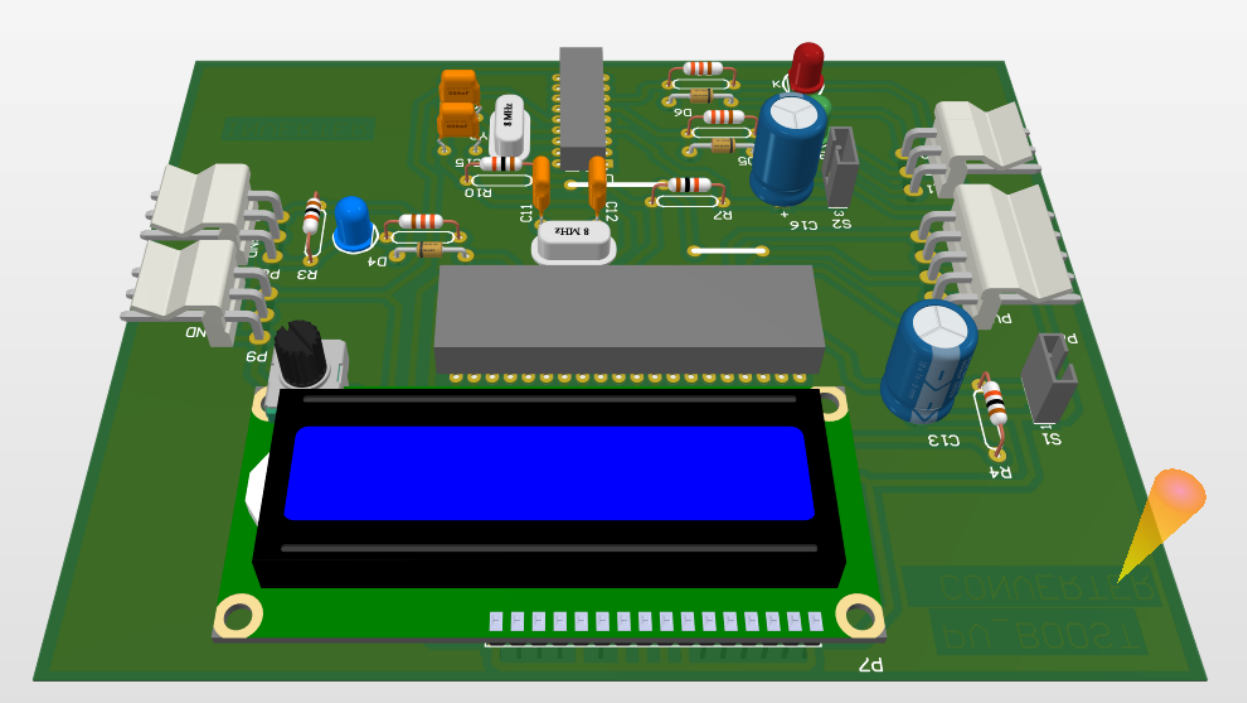

Fig.III.12b. The 3D layout of the Booster controller PCB

Below is the fully designed electronic control card for the DC-DC booster.

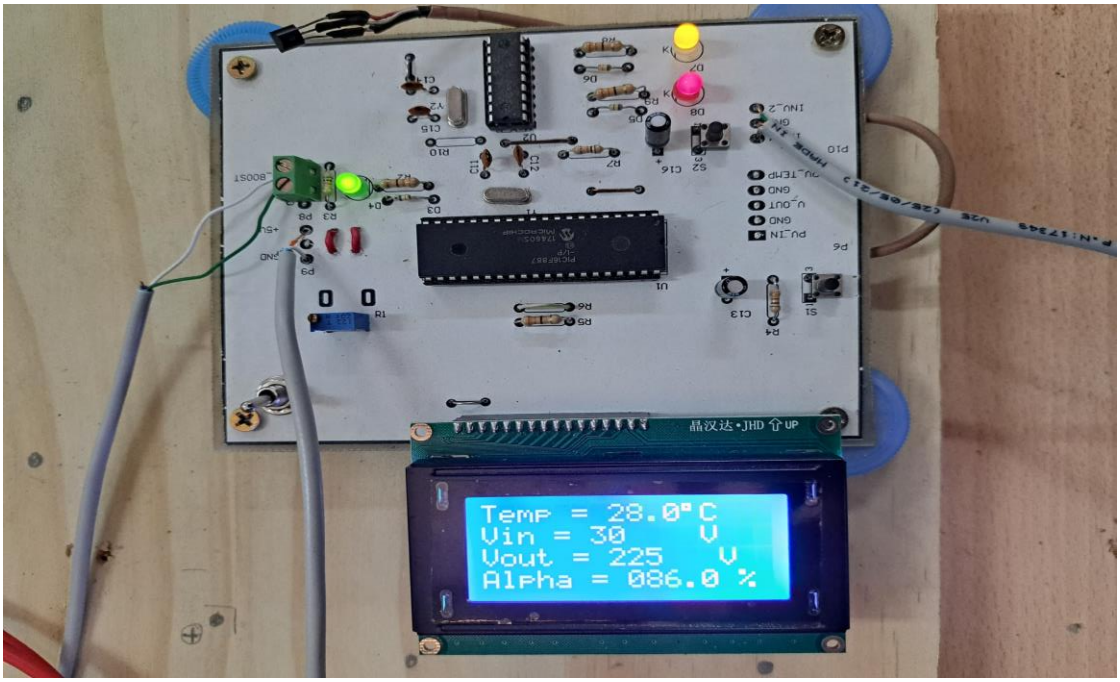

Fig III.13. The printed booster control card

On testing the control card in the laboratory, we obtained the following curves in figures III.14a, b & c from the oscilloscope indicating the three different duty cycles generated from the boost control card. The blue signal is the signal directly from the PIC16F887 and the yellow one is captured at the output of the driver IR2110 after calibration. We notice that the one at the output of the driver is amplified which is one of the roles of the mosfet driver IR2110.

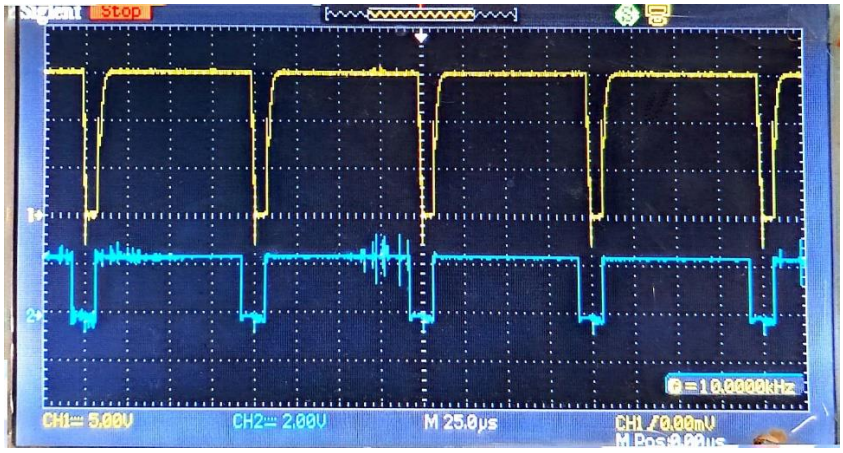

Fig.III.14a. Duty cycle signal of 86%

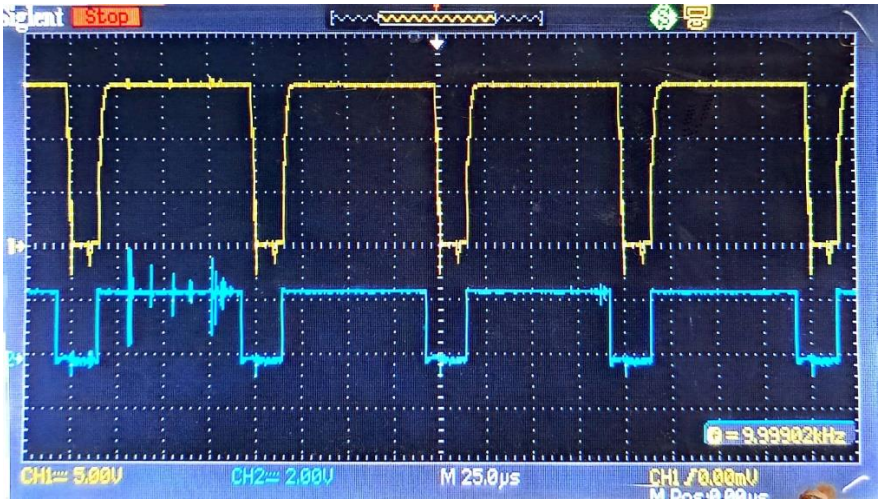

Fig.III.14b. Duty cycle signal of 83%.

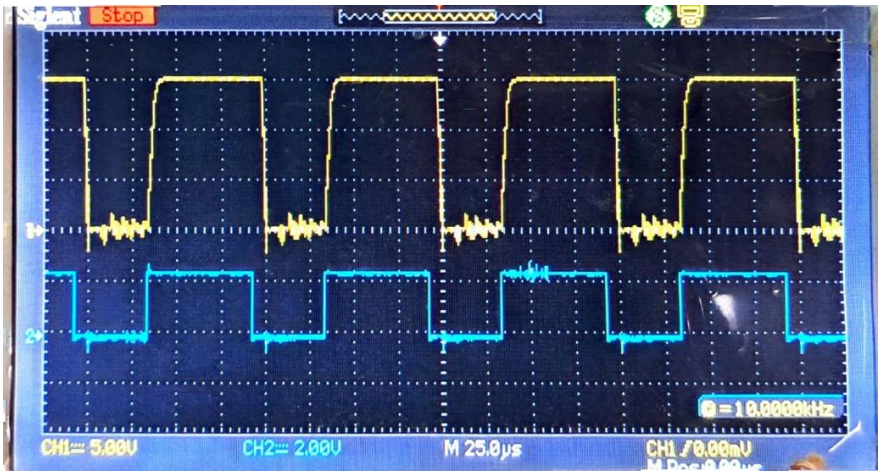

Fig.III.14c. Duty cycle signal of 80%.

III.5.2. Design and implementation of the DC-DC Booster electronic card

We constructed a DC-DC booster using Altium Designer. Figure III.15 shows a schematic diagram of our boost converter in Altium designer software.

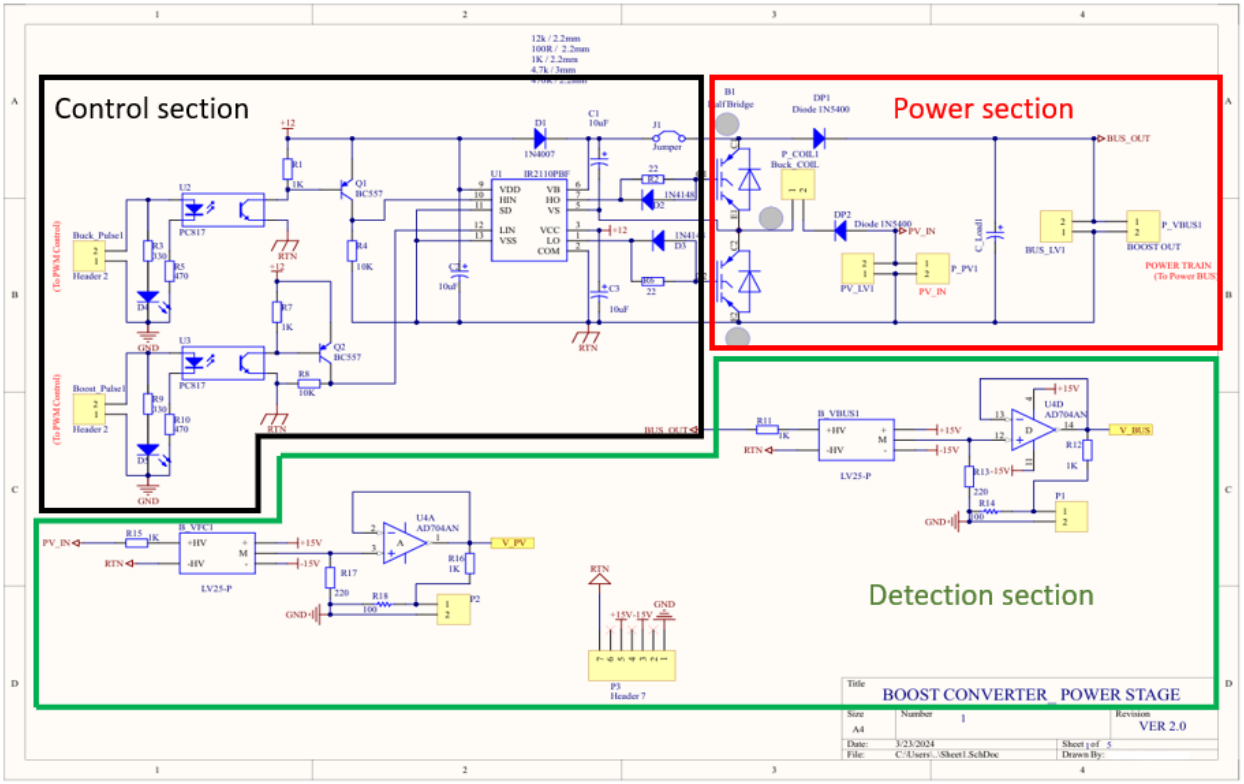

Fig III.15. Schematic diagram of the DC-DC Boost converter

The schematic is made up of three sections namely; detection, control and power section. It is strategically organized in sections for electrical protection and to make trouble shooting easier in case of a faulty component.

- **The detection section**

Among the components in this section, are two voltage sensors namely LV-25P. These provide measurement of the input and output voltages of the booster which are used to calculate the duty cycle, α as explained in the previous chapter. They also provide galvanic isolation of the microcontroller. Another important component is the AD704AN which is used to regulate the measured voltage values before being injected into the microcontroller. The datasheets of these components are attached in the appendix in figure A10 and figure A8 respectively.

- **The control section**

The control section receives the generated duty cycle(signal) from the microcontroller. It is comprised of treatment and protection components among which are two optocouplers and an IR2110 driver. The optocouplers are used for electrical isolation and protection of the microcontroller Their data sheet is represented in figure A2 and A3 of the appendix. The IR2110 amplifies and calibrates the signal so as to attack the transistors. It also calculates the dead time between the commutation of the two transistors on the same branch to avoid a short circuit. The driver's datasheet is provided in figure A6 of the appendix.

- **The power section**

Our DC-DC converter is universal therefore we designed it as a buck-boost converter although in our application we strictly use it as a boost converter. It's for this reason we used two transistors instead of a single transistor and a diode. The SKM 100GB123D IGBT branch we used has its datasheet represented in figure A1 of the appendix. We used an inductor coil of 330μH and a filtering capacitor of 3.4μF.

We then simulated the DC-DC booster schematic in MATLAB Simulink and we obtain the following graph in figure III.16. At 86% duty cycle we obtained a 230V DC output as shown in the figure below.

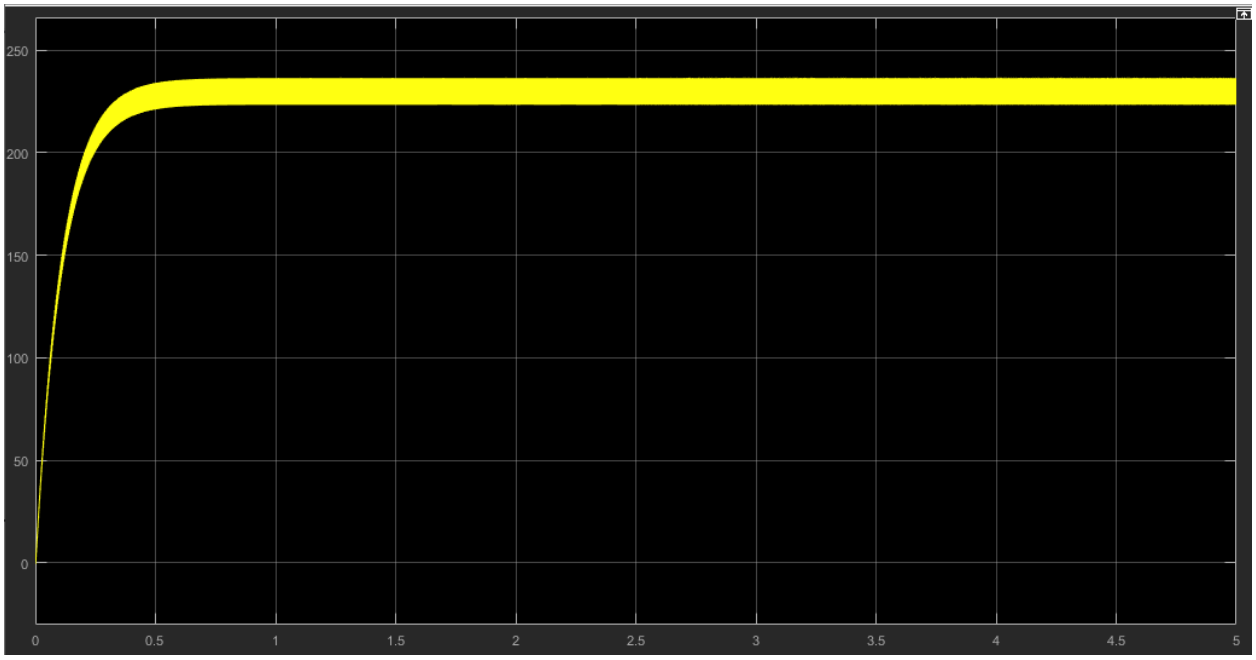

Fig. III.16. Simulation output voltage curve for the DC

A minimal number of ripples is observed in the waveform of output voltage above. This relative ripple is of 5.6% of the mean output voltage value. The figure III.16 below shows a magnified voltage waveform depicting the ripples in the voltage.

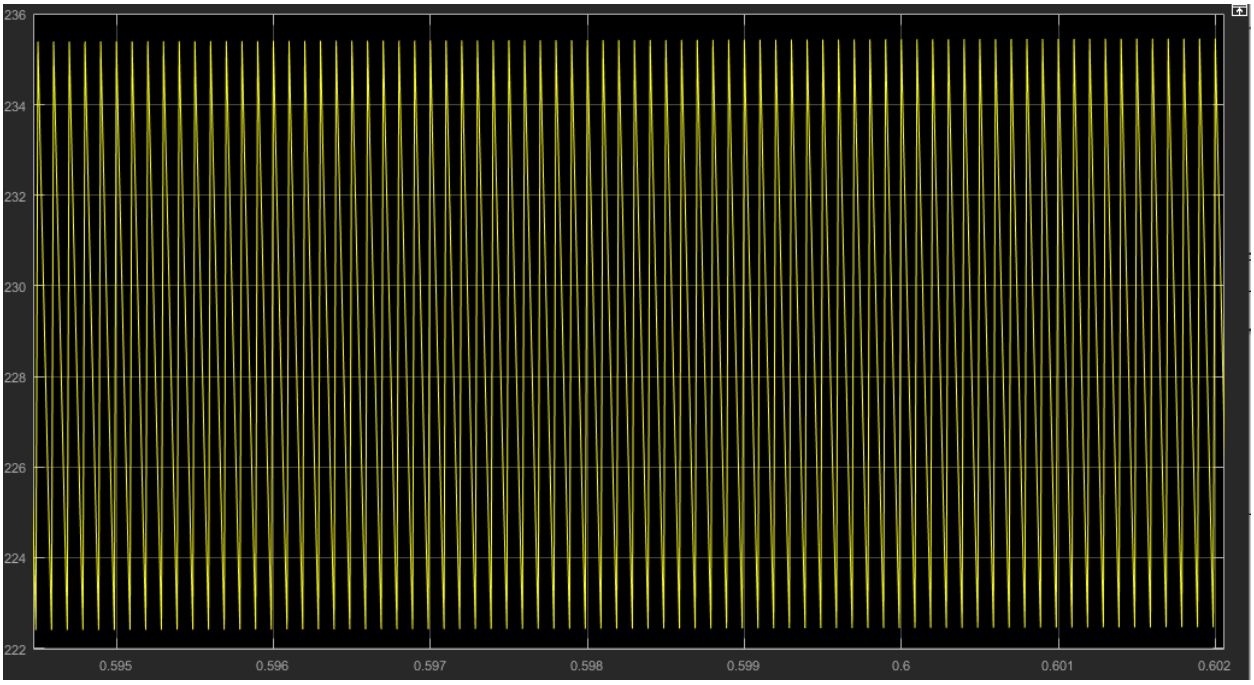

Fig III.17. Ripples in the DC-DC booster output voltage.

From the above schematic in fig III.15, we designed a PCB circuit using each component's footprint which is shown in fig III.18a & b below.

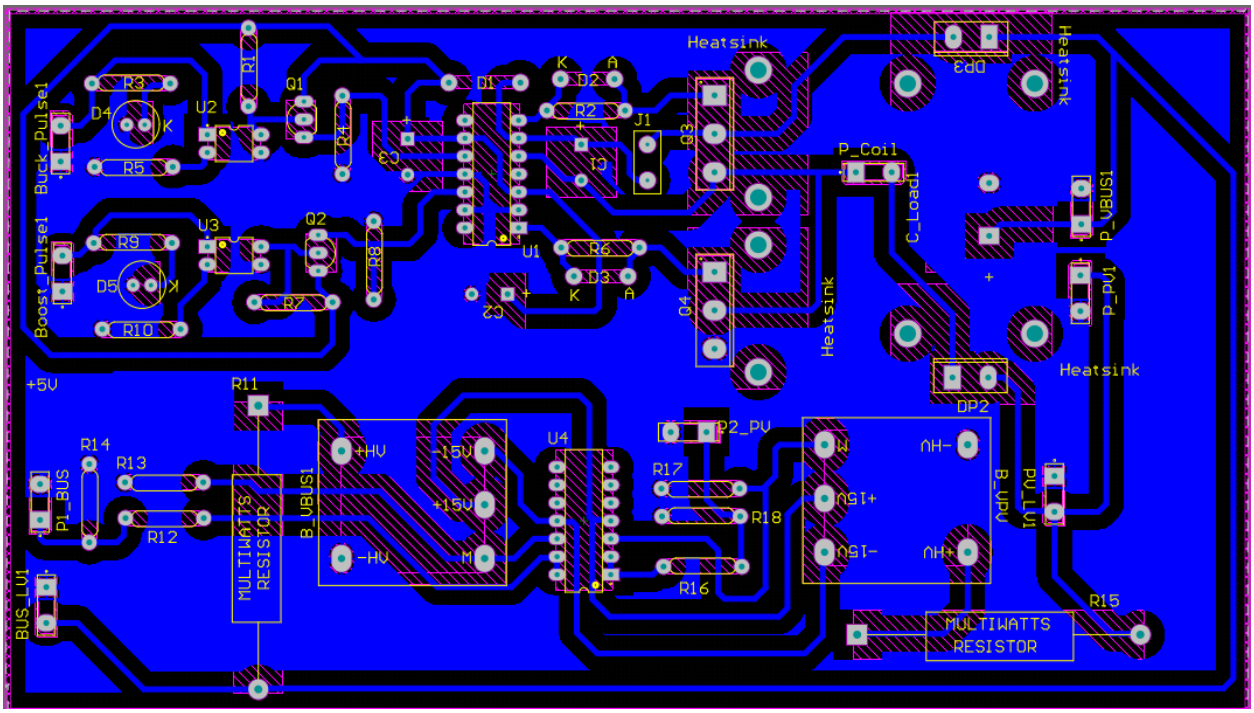

Fig III.18a. 2D PCB design of the DC-DC booster

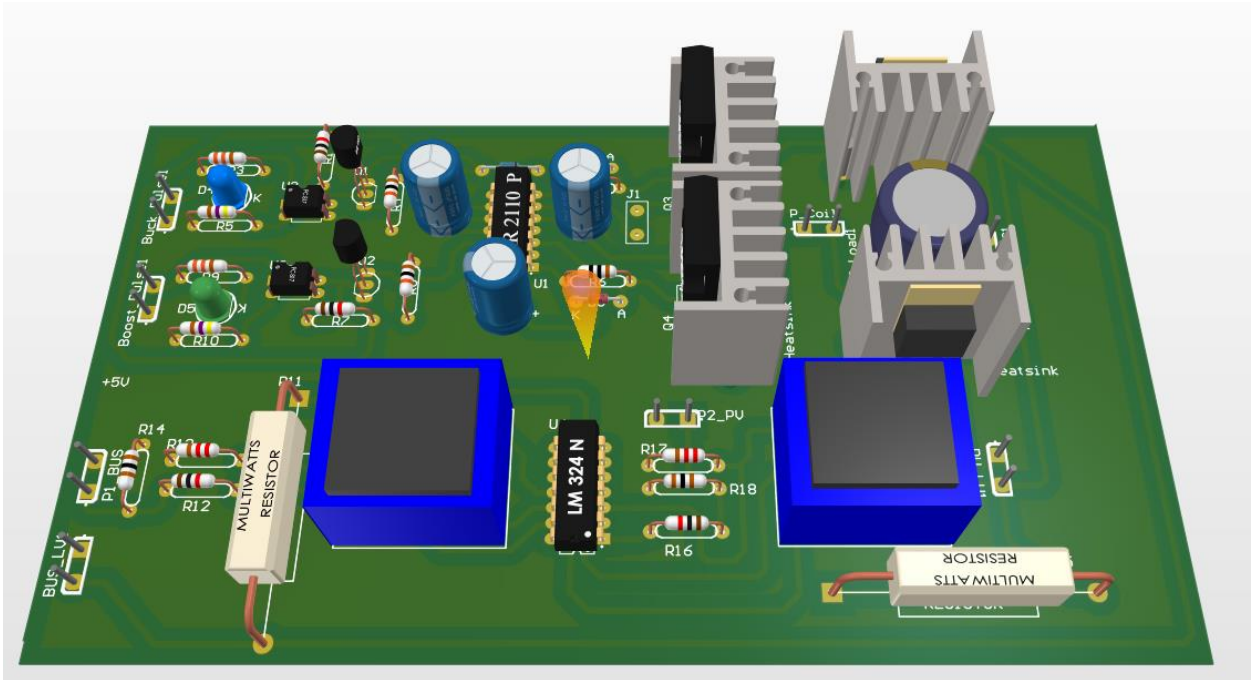

Fig III.18b. 3D PCB design of the DC-DC booster

Below is the final printed circuit board of our DC-DC boost in figure III.19.

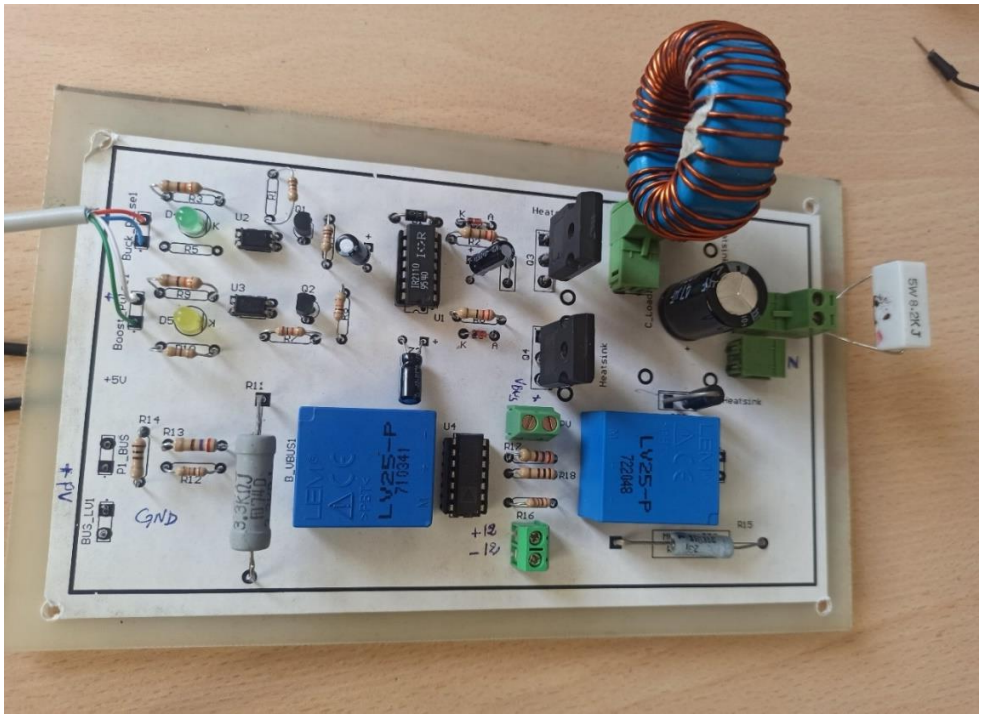

Fig III.19. The printed circuit board of the DC-DC booster

We equally ran lab tests on our DC-DC booster and the respective output voltages with the different duty cycles were obtained as shown in fig III.20a, b & c below. Each division is 10 x 10V.

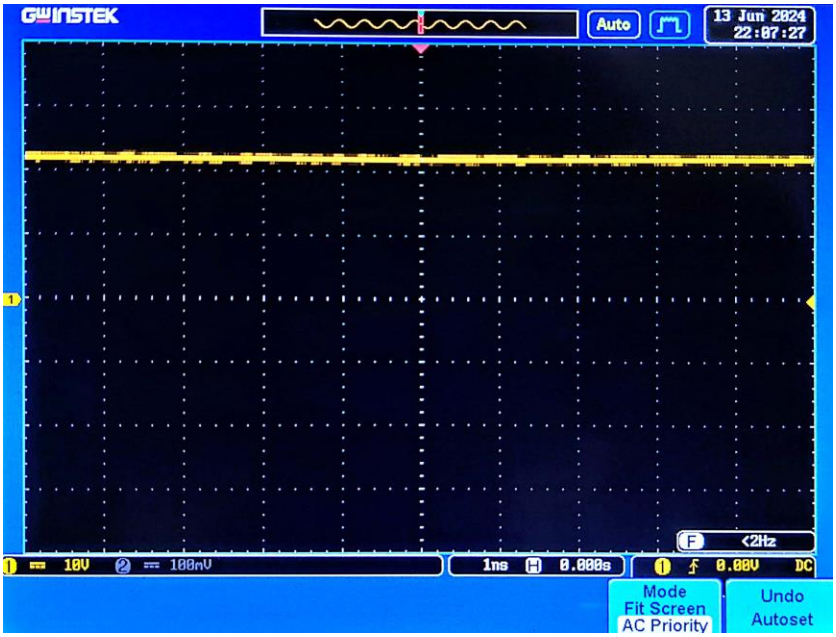

Fig III.20a. 230V output voltage curve of the DC-DC booster.

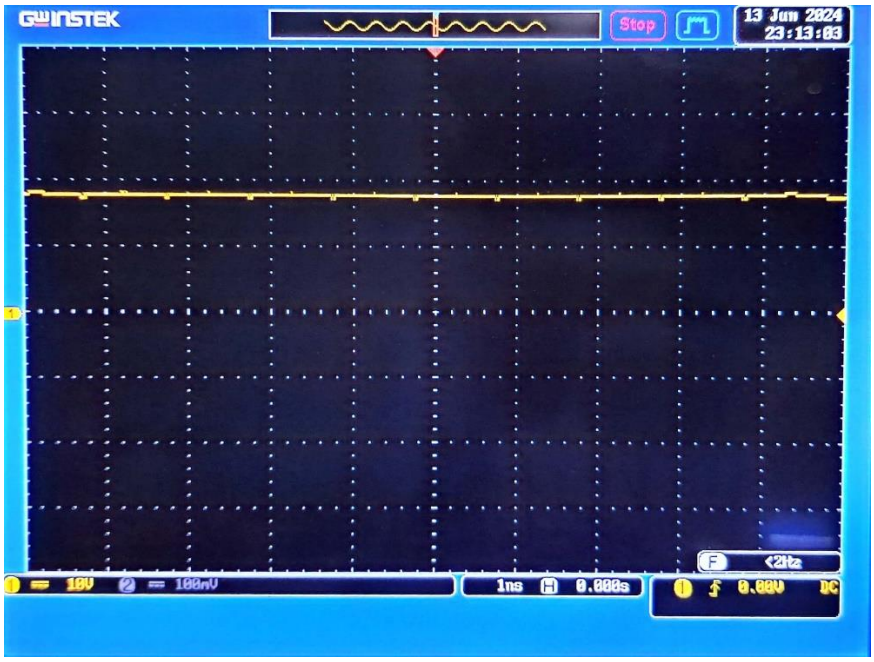

Fig III.20b. 180V output voltage curve of the DC-DC booster.

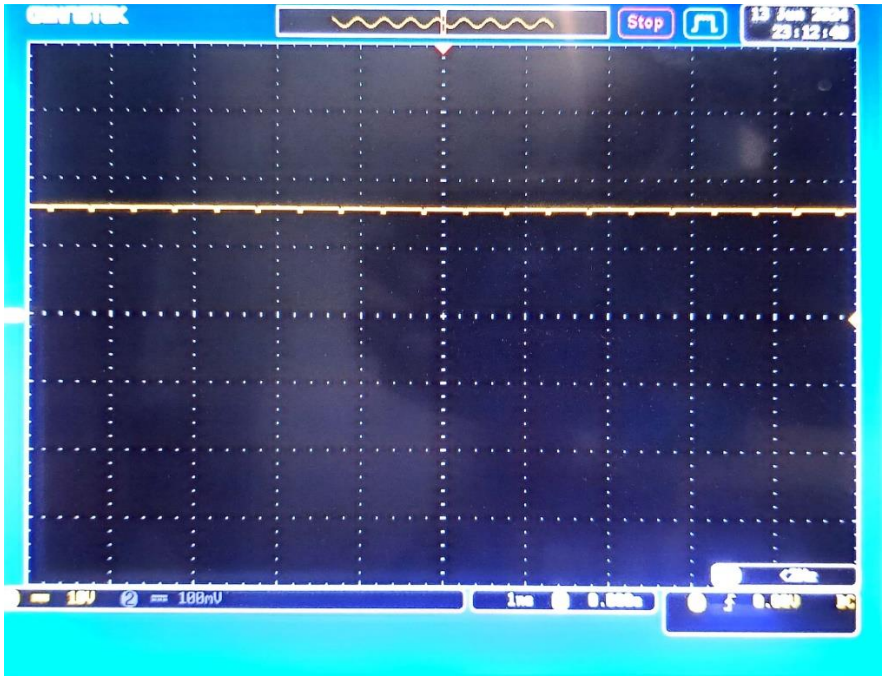

Fig III.20c. 150V output voltage curve of the DC-DC booster.

Figure III.21 below shows the whole laboratory set-up while we ran tests of the designed cards.

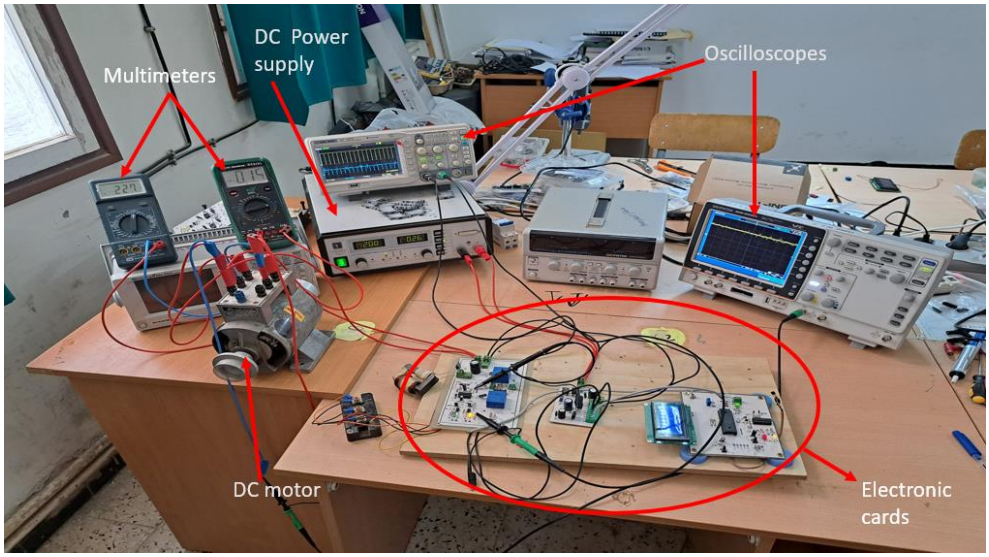

Fig III.21. Laboratory set-up showing designed components

III.6. The overall system

After having designed the electronic power converter plus its support electronic cards, we now feed them back into our global system so as to attain our main goal of powering the water fountain from a 30V source of the solar panels. In so doing, we shall give a detailed description of the rest of our project components.

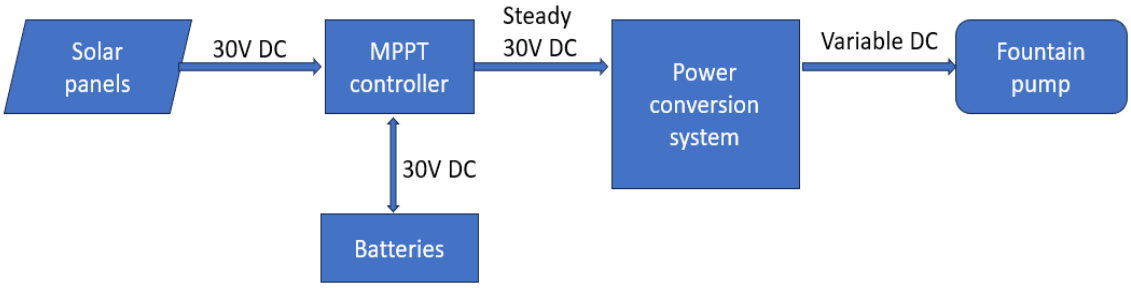

Fig III.22. The overall system

III.6.1. Solar panels

We used a 4P configuration of solar panels that is, 4 panels in parallel. Each solar panel has a maximum output power output of 315W, maximum current output of 9.49A and maximum voltage output of 33.2V

Table 1: The characteristics of one PV module

Maximum power	**315W**
Power tolerance	**0 ~ +3%**
Maximum power voltage (Vmp)	**33.2V**
Maximum power current (Imp)	**9.49A**
Open circuit voltage (Voc)	**40.7V**
Short circuit current (Isc)	**10.04A**
Operating Temperature	**-40 ~ +80ºC**

III.6.2. MPPT controller

We used an Epever Tracer4210AN rated 40A/100V maximum output. This controller is internally configured as showed in figure III.23. There is a buck or boost converter configuration in between every two elements i.e. solar panel, batteries and load depending on the voltage values needed.

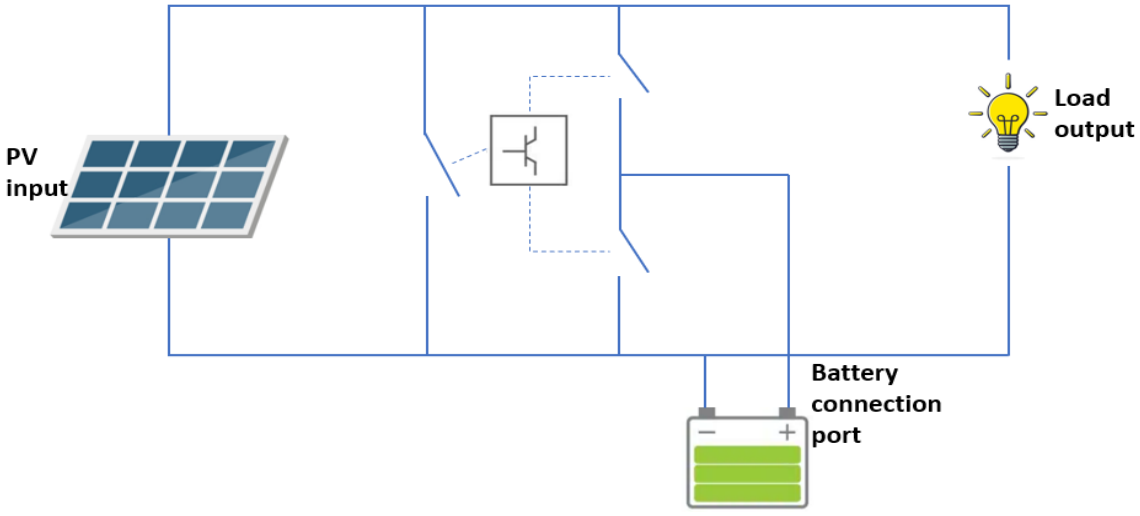

Fig III.23. MPPT controller electrical configuration

The controller receives 30V DC from the solar panels from which it charges our battery setup at 30V and provides a 30V load supply to the DC-DC boost converter.

Fig III.24. Epever MPPT controller

III.6.3. Batteries

We used two lithium batteries in series. Each battery has a voltage of 15V which equals to a total of 30V. These batteries assume the role of powering the load when there's low energy values from the solar panels hence providing reliability of power to the load.

Fig III.25. Set of lithium batteries used in this project

From the steady 30V DC at the output of the MPPT controller we generated an interval of 150V - 230V DC. To do that, we used a DC-DC boost converter which we designed as explained

above in ***III.5. Design and implementation the DC-DC booster converter.*** At this stage we are ready to power the water pump that supplies our fountain.

III.6.4. Fountain pump

For the motor-pump set, we found application in the Lucas-Nuelle Lehr DC motor rated 0.2KW and 220-240V power supply coupled with a single turbine centrifugal pump, with a maximum water head of 40m which is more than enough for our fountain.

Table 2: Characteristic properties of the motor-pump

Nominal current (In)	**1.2 A**
Voltage input	**220 – 240V**
Power output	**0.2KW**
Motor speed	**2000 rpm**
Flow rate	**5 – 35 liter/min**
Temperature	**40 ºC**
Hmin	**5m**
Hmax	**40m**

Figure III.26 below shows the fully functional water fountain at the faculty of technology UMBB

Fig III.26. The water fountain at the Project site

III.7. Conclusion

In conclusion, this chapter has provided a thorough exploration of our PVWPS, highlighting the integration and functionality of key components like the boost converter and its support electronic cards. We have demonstrated how these elements work together under the management of the control card to achieve efficient energy conversion and system stability. The detailed insights into our system's architecture and operational principles underscore our project's innovative approach to sustainable water pumping solutions, displaying its potential to address real-world challenges effectively.

GENERAL CONCLUSION

GENERAL CONCLUSION

In this thesis, we have designed and implemented a Photovoltaic Water Pumping System (PVWPS) intended to supply a fountain at the Faculty of Technology of UMBB. This comprehensive endeavor began with an exploration of the general principles of PVWPS, where we delved into their definitions, types, and installation procedures, among other relevant topics.

Our initial focus was on understanding the broader aspects of PVWPS to lay a solid foundation for the project. We then concentrated on the power converters and their modeling, with a particular emphasis on DC-DC converters, specifically choppers in boost mode. This choice was driven by the necessity of using a boost converter in our project to step up the voltage from the photovoltaic panels.

The third and final chapter detailed the design and implementation of the PVWPS for our faculty's fountain. The system primarily consists of a DC-DC boost converter and its control card. This boost converter steps up the 30 V from the solar panels to three different voltage levels, corresponding to three distinct water head heights of the fountain, thus demonstrating the system's versatility and efficiency.

Looking ahead, we envisage several enhancements to this project. One of our primary goals is to design and integrate a single-phase inverter alongside the DC-DC boost converter. This integration will enable the system to run an induction motor, which is generally more efficient and reliable than a DC motor for such applications.

For future researchers and developers aiming to build upon this project, there are several valuable directions to consider. First, incorporating mobile orientation for the solar panels to track the sun's position throughout the day could significantly improve the photovoltaic power output. This dynamic adjustment would optimize the panels' exposure to sunlight, thereby enhancing the system's overall efficiency.

Additionally, a thorough re-evaluation and improvement of the hydraulic system's design and dimensioning would be beneficial. This includes optimizing the number of turbines and the length of the motor section to maximize the water pump's output power. Such refinements would

not only improve the system's performance but also ensure its long-term sustainability and reliability.

In conclusion, this thesis has successfully demonstrated the feasibility and practicality of using a PVWPS to supply a water fountain. Through meticulous design and implementation, we have created a system that not only meets the current needs but also offers a clear pathway for future improvements. The proposed enhancements, if implemented, will further elevate the system's efficiency and broaden its applicability, paving the way for more advanced and sustainable water pumping solutions.

REFERENCES

REFERENCES

[1] Khatib, T., Mohamed, A., & Sopian, K. (2013). A review of photovoltaic systems size optimization techniques. *Renewable and Sustainable Energy Reviews*, *22*, 454-465.

[2] Khatib, T., Ibrahim, I. A., & Mohamed, A. (2016). A review on sizing methodologies of photovoltaic array and storage battery in a standalone photovoltaic system. *Energy Conversion and Management*, *120*, 430-448.

[3] Kaplani, E., & Kaplanis, S. (2012). A stochastic simulation model for reliable PV system sizing providing for solar radiation fluctuations. *Applied Energy*, *97*, 970-981.

[4] Acakpovi, A., Xavier, F. F., & Awuah-Baffour, R. (2012, October). Analytical method of sizing photovoltaic water pumping system. In *2012 IEEE 4th International Conference on Adaptive Science & Technology (ICAST)* (pp. 65-69). IEEE.

[5] Campana, P. E., Li, H., & Yan, J. (2013). Dynamic modelling of a PV pumping system with special consideration on water demand. *Applied energy*, *112*, 635-645.

[6] Moulay-Idriss, C., & Mohamed, B. (2013). Application of the DTC control in the photovoltaic pumping system. *Energy Conversion and Management*, *65*, 655-662.

[7] Raveendhra, D., Joshi, P., & Verma, R. K. (2014, March). Performance and control system design for FPGA based CVMPPT boost converter for remote SPV water pumping system applications. In *2014 POWER AND ENERGY SYSTEMS: TOWARDS SUSTAINABLE ENERGY* (pp. 1-6). IEEE.

[8] Alnaqi, A. A., Moayedi, H., Shahsavar, A., & Nguyen, T. K. (2019). Prediction of energetic performance of a building integrated photovoltaic/thermal system thorough artificial neural network and hybrid particle swarm optimization models. *Energy conversion and management*, *183*, 137-148.

[9] Liu, H., Khan, M. Y. A., & Yuan, X. (2023). Hybrid maximum power extraction methods for photovoltaic systems: a comprehensive review. *Energies*, *16*(15), 5665.

[10] MP, V., & Anand, B. (2020). Particle swarm optimization technique for multilevel inverters in solar harvesting micro grid system.

[11] Kamarzaman, N. A., & Tan, C. W. (2014). A comprehensive review of maximum power point tracking algorithms for photovoltaic systems. *Renewable and Sustainable Energy Reviews*, *37*, 585-598.

[12] Ahmed, J., & Salam, Z. (2018). An enhanced adaptive P&O MPPT for fast and efficient tracking under varying environmental conditions. *IEEE Transactions on Sustainable Energy*, *9*(3), 1487-1496.

[13] Andoulssi, R., Draou, A., Jerbi, H., Alghonamy, A., & Khiari, B. (2013). Nonlinear control of a photovoltaic water pumping system. *Energy Procedia*, *42*, 328-336.

[14] Katan, R. E., Agelidis, V. G., & Nayar, C. V. (1996, January). Performance analysis of a solar water pumping system. In *Proceedings of International Conference on Power Electronics, Drives and Energy Systems for Industrial Growth* (Vol. 1, pp. 81-87). IEEE.

[15] Elgendy, M. A., Zahawi, B., & Atkinson, D. J. (2011). Assessment of perturb and observe MPPT algorithm implementation techniques for PV pumping applications. *IEEE transactions on sustainable energy*, *3*(1), 21-33.

[16] Alghuwainem, S. M. (1992). Steady-state performance of DC motors supplied from photovoltaic generators with step-up converter. *IEEE Transactions on Energy Conversion*, *7*(2), 267-272.

[17] Khatib, T., & Muhsen, D. H. (2020). *Photovoltaic water pumping systems: concept, design, and methods of optimization*. Academic Press.

[18] Discount Pumps. (2024). *How to Choose a Fountain, Aerator or Pump for your Pond.* https://discount-pumps.biz/choose-pond-pump.htm

[19] Africa Clean Energy Technical Assistance Facility. (2019). *Uganda Solar Water Pumping Report*. https://ace-taf.org/kb/uganda-solar-water-pumping-report/

[20] Arab, A. H., Chenlo, F., Mukadam, K., & Balenzategui, J. L. (1999). Performance of PV water pumping systems. *Renewable Energy*, *18*(2), 191-204.

[21] Mohammedi, A., Mezzai, N., Rekioua, D., & Rekioua, T. (2014). Impact of shadow on the performances of a domestic photovoltaic pumping system incorporating an MPPT control: A case study in Bejaia, North Algeria. *Energy Conversion and Management*, *84*, 20-29.

[22] Benghanem, M., Daffallah, K. O., Joraid, A. A., Alamri, S. N., & Jaber, A. (2013). Performances of solar water pumping system using helical pump for a deep well: A case study for Madinah, Saudi Arabia. *Energy Conversion and Management*, *65*, 50-56.

[23] Smith, J. (2021). *Advanced power converters for photovoltaic applications in water pumping systems* (Doctoral dissertation). Massachusetts Institute of Technology.

[24] Bordry, F. (2006). Power converters: definitions, classification and converter topologies.

[25] Trzynadlowski, A. M. (2015). *Power electronic converters and systems: Frontiers and applications* (No. 10849). IET

[26] Gui, Y., Blaabjerg, F., Wang, X., Bendtsen, J. D., Yang, D., & Stoustrup, J. (2020). Improved DC-link voltage regulation strategy for grid-connected converters. *IEEE Transactions on Industrial Electronics*, *68*(6), 4977-4987.

[27] de Azpeitia, M. A. P. (2021). *Design and Control of Power Converters 2020* (p. 188). MDPI-Multidisciplinary Digital Publishing Institute.

[28] Vodovozov, V., & Jansikene, R. (2006). *Power electronic converters*.

[29] Kumar, L. A., Alexander, S. A., & Rajendran, M. (2020). *Power electronic converters for solar photovoltaic systems*. Academic Press.

[30] Forrisi, I. (2016). *Contribution aux systèmes renouvelables connectés en réseau : contrôle, analyse de la stabilité et fiabilité* (Doctoral dissertation, Université de Lorraine).

APPENDICES

SKM 100GB123D

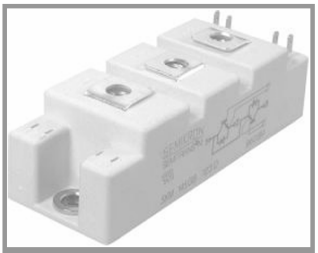

SEMITRANS® 2

IGBT Modules

SKM 100GB123D
SKM 100GAL123D
SKM 100GAR123D

Features

- MOS input (voltage controlled)
- N channel, Homogeneous Si
- Low inductance case
- Very low tail current with low temperature dependence
- High short circuit capability, self limiting to 6 x I_{cnom}
- Latch-up free
- Fast & soft inverse CAL diodes
- Isolated copper baseplate using DCB Direct Copper Bonding Technology
- Large clearance (10 mm) and creepage distances (20 mm)

Typical Applications

- AC inverter drives
- UPS

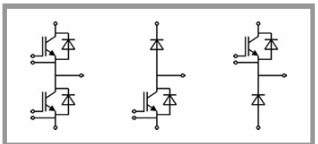

GB GAL GAR

Absolute Maximum Ratings T_c = 25 °C, unless otherwise specified

Symbol	Conditions		Values	Units
IGBT				
V_{CES}	T_j = 25 °C		1200	V
I_C	T_j = 150 °C	T_{case} = 25 °C	100	A
		T_{case} = 80 °C	90	A
I_{CRM}	I_{CRM}=2xI_{Cnom}		150	A
V_{GES}			± 20	V
t_{psc}	V_{CC} = 600 V; $V_{GE} \leq$ 20 V; V_{CES} < 1200 V	T_j = 125 °C	10	µs
Inverse Diode				
I_F	T_j = 150 °C	T_{case} = 25 °C	95	A
		T_{case} = 80 °C	65	A
I_{FRM}	I_{FRM}=2xI_{Fnom}		150	A
I_{FSM}	t_p = 10 ms; sin.	T_j = 150 °C	720	A
Freewheeling Diode				
I_F	T_j = 150 °C	T_{case} = 25 °C	130	A
		T_{case} = 80 °C	90	A
I_{FRM}	I_{FRM}=2xI_{Fnom}		200	A
I_{FSM}	t_p = 10 ms; sin.	T_j = 150 °C	900	A
Module				
$I_{t(RMS)}$			200	A
T_{vj}			- 40... + 150	°C
T_{stg}			- 40...+ 125	°C
V_{isol}	AC, 1 min.		2500	V

Characteristics T_c = 25 °C, unless otherwise specified

Symbol	Conditions		min.	typ.	max.	Units
IGBT						
$V_{GE(th)}$	V_{GE} = V_{CE}, I_C = 2 mA		4,5	5,5	6,5	V
I_{CES}	V_{GE} = 0 V, V_{CE} = V_{CES}	T_j = 25 °C		0,1	0,3	mA
V_{CE0}		T_j = 25 °C		1,4	1,6	V
		T_j = 125 °C		1,6	1,8	V
r_{CE}	V_{GE} = 15 V	T_j = 25°C		14,6	18,6	mΩ
		T_j = 125°C		20	25,3	mΩ
$V_{CE(sat)}$	I_{Cnom} = 75 A, V_{GE} = 15 V	T_j = °$C_{chiplev.}$		2,5	3	V
C_{ies}	V_{CE} = 25, V_{GE} = 0 V	f = 1 MHz		5	6,6	nF
C_{oes}				0,72	0,9	nF
C_{res}				0,38	0,5	nF
Q_G	V_{GE} = -8V - +20V			750		nC
R_{Gint}	T_j = °C			5		Ω
$t_{d(on)}$	R_{Gon} = 15 Ω	V_{CC} = 600V		30	60	ns
t_r		I_{Cnom} = 75A		70	140	ns
E_{on}		T_j = 125 °C		10		mJ
$t_{d(off)}$	R_{Goff} = 15 Ω	V_{GE} = ± 15V		450	600	ns
t_f				70	90	ns
E_{off}				8		mJ
$R_{th(j-c)}$	per IGBT				0,18	K/W

Figure A1: 1st page of the data sheet of the IGBT branch

PC817 Series

High Density Mounting Type Photocoupler

❋ Lead forming type（I type ）and taping reel type （P type ）are also available.（**PC817I/PC817P** ）
❋❋ TÜV（VDE0884 ）approved type is also available as an option.

■ Features

1. Current transfer ratio
（CTR: MIN. 50% at I_F = 5mA ,V_{CE}=5V)
2. High isolation voltage between input and output（V_{iso}： 5 000V_{rms}）
3. Compact dual-in-line package
PC817： 1-channel type
PC827： 2-channel type
PC837： 3-channel type
PC847： 4-channel type
4. Recognized by UL, file No. E64380

■ Applications

1. Computer terminals
2. System appliances, measuring instruments
3. Registers, copiers, automatic vending machines
4. Electric home appliances, such as fan heaters, etc.
5. Signal transmission between circuits of different potentials and impedances

■ Outline Dimensions

（Unit： mm）

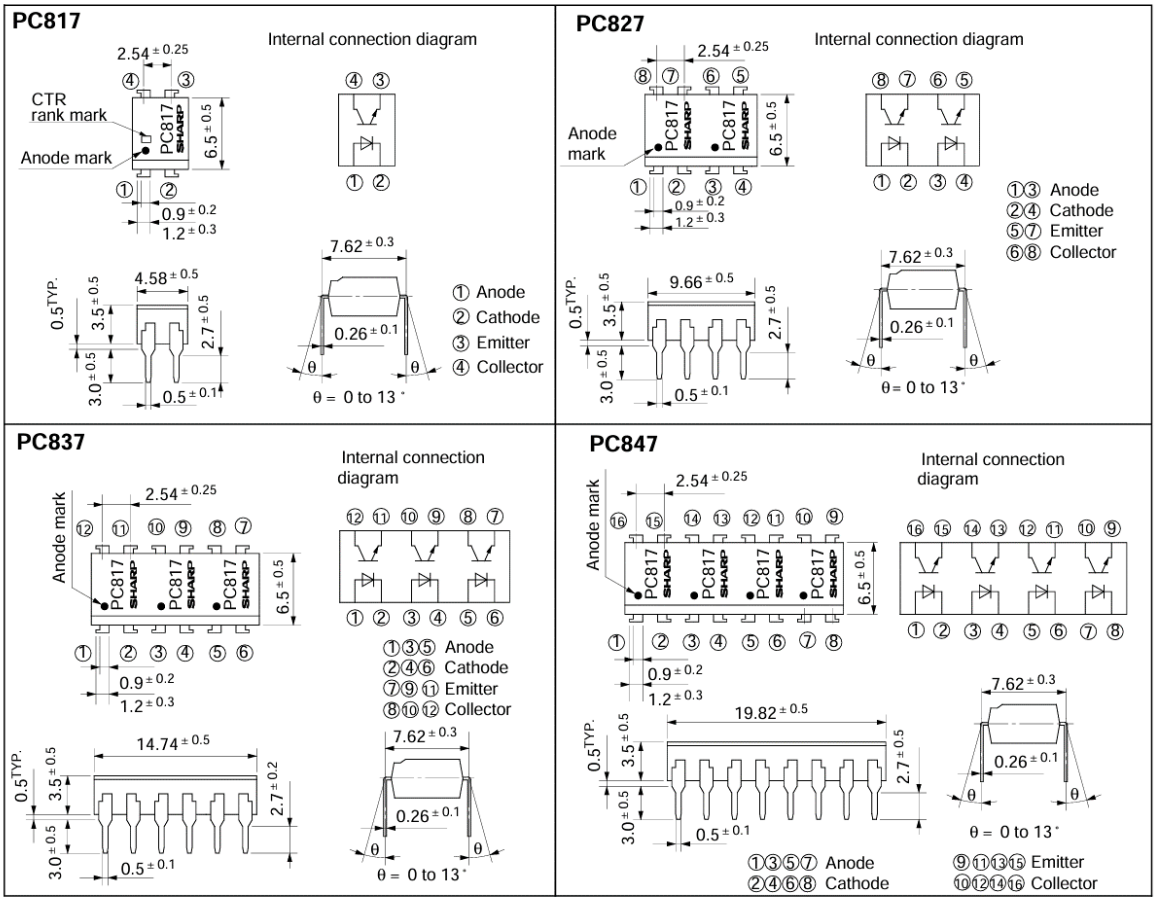

Figure A2: 1st page of the data sheet of the opto-coupler

■ Absolute Maximum Ratings (Ta= 25°C)

Parameter		Symbol	Rating	Unit
Input	Forward current	I_F	50	mA
	*1Peak forward current	I_{FM}	1	A
	Reverse voltage	V_R	6	V
	Power dissipation	P	70	mW
Output	Collector-emitter voltage	V_{CEO}	35	V
	Emitter-collector voltage	V_{ECO}	6	V
	Collector current	I_C	50	mA
	Collector power dissipation	P_C	150	mW
Total power dissipation		P_{tot}	200	mW
*2Isolation voltage		V_{iso}	5 000	V_{rms}
Operating temperature		T_{opr}	- 30 to + 100	°C
Storage temperature		T_{stg}	- 55 to + 125	°C
*3Soldering temperature		T_{sol}	260	°C

*1 Pulse width <=100μs, Duty ratio : 0.001
*2 40 to 60% RH, AC for 1 minute
*3 For 10 seconds

■ Electro-optical Characteristics (Ta= 25°C)

Parameter			Symbol	Conditions	MIN.	TYP.	MAX.	Unit
Input	Forward voltage		V_F	I_F = 20mA	-	1.2	1.4	V
	Peak forward voltage		V_{FM}	I_{FM} = 0.5A	-	-	3.0	V
	Reverse current		I_R	V_R = 4V	-	-	10	μA
	Terminal capacitance		C_t	V = 0, f = 1kHz	-	30	250	pF
Output	Collector dark current		I_{CEO}	V_{CE} = 20V	-	-	10^{-7}	A
Transfer characteristics	*4Current transfer ratio		CTR	I_F = 5mA, V_{CE} = 5V	50	-	600	%
	Collector-emitter saturation voltage		$V_{CE(sat)}$	I_F = 20mA, I_C = 1mA	-	0.1	0.2	V
	Isolation resistance		R_{ISO}	DC500V, 40 to 60% RH	5×10^{10}	10^{11}	-	Ω
	Floating capacitance		C_f	V = 0, f = 1MHz	-	0.6	1.0	pF
	Cut-off frequency		f_c	V_{CE} = 5V, I_C = 2mA, R_L = 100Ω, - 3dB	-	80	-	kHz
	Response time	Rise time	t_r	V_{CE} = 2V, I_C = 2mA, R_L = 100Ω	-	4	18	μs
		Fall time	t_f		-	3	18	μs

*4 Classification table of current transfer ratio is shown below.

Model No.	Rank mark	CTR (%)
PC817A	A	80 to 160
PC817B	B	130 to 260
PC817C	C	200 to 400
PC817D	D	300 to 600
PC8✵7AB	A or B	80 to 260
PC8✵7BC	B or C	130 to 400
PC8✵7CD	C or D	200 to 600
PC8✵7AC	A, B or C	80 to 400
PC8✵7BD	B, C or D	130 to 600
PC8✵7AD	A, B, C or D	80 to 600
PC8✵7	A, B, C, D or No mark	50 to 600

✵ : 1 or 2 or 3 or 4

Fig. 1 Forward Current vs. Ambient Temperature

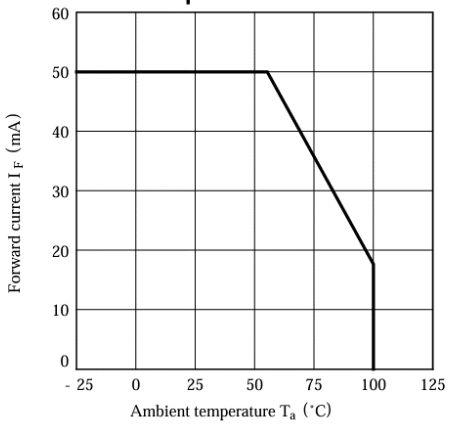

Figure A3: 2nd page of the data sheet of the opto-coupler

Electrical characteristics 7805

Electrical characteristics at specified virtual junction temperature, V= 10V, Io = 500mA (unless otherwise noted)

Parameter	Test Conditions*		7805			Units
			Min	Typ	Max	
Output voltage**		25C	4.8	5	5.2	V
	Io= 5mA to 1A, V= 7V to 20V, P≤ 15W	0C to 125C	4.75	5	5.25	
Input regulation		25C		3	100	mV
	V= 7V to 25V			1	50	
Ripple rejection	V= 8V to 18V, f= 120Hz	0C to 125C	62	78		dB
Output regulation	Io= 5mA to 1.5A	25C		15	100	mV
	Io= 250mA to 750mA			5	50	
Output resistance	f= 1KHz	0C to 125C		0.017		Ω
Temperature coefficient of output voltage	Io= 5mA	0C to 125C		-1.1		mV/C
Output noise voltage	f= 10 Hz to 100 KHz	25C		40		μV
Dropout voltage	Io= 1A	25C		2.0		V
Bias current		25C		4.2	8	mA
Bias current change	V= 7V to 25V	0C to 125C			1.3	
	Io= 5mA to 1A				0.5	
Short-circuit output current		25C		750		
Peak output current		25C		2.2		A

* Pulse testing techniques are used to maintain the junction temperature as close to the ambient temperature as possible. Thermal effects must be taken into account separately.

** This specification applies only for dc power dissipation permitted by absolute maximum ratings.

Figure A4: Data sheet of the 7805 voltage regulator

Electrical Characteristics 7815

Electrical characteristics at specified virtual junction temperature, V= 23V, Io = 500mA (unless otherwise noted)

Parameter	Test Conditions*		MIK7815			Units
			Min	Typ	Max	
Output voltage**		25C	14.4	15	15.6	V
	Io= 5mA to 1A, V= 17.5V to 30V, P≤	0C to 125C	14.25	15	15.75	
Input regulation	V= 17.5V to 30V	25C		12	300	mV
	V= 20V to 26V			3	150	
Ripple rejection	V= 18.5V to 28.5V, f= 120Hz	0C to 125C	54	70		dB
Output regulation	Io= 5mA to 1.5A	25C		12	300	mV
	Io= 250mA to 750mA			4	150	
Output resistance	f= 1KHz	0C to 125C		0.019		Ω
Temperature coefficient of output voltage	Io= 5mA	0C to 125C		-1.0		mV/C
Output noise voltage	f= 10 Hz to 100 KHz	25C		90		μV
Dropout voltage	Io= 1A	25C		2.0		V
Bias current		25C		4.3	8	
Bias current change	V= 17.5V to 30V	0C to 125C			1	mA
	Io= 5mA to 1A				0.5	
Short-circuit output current		25C		230		
Peak output current		25C		2.1		A

Figure A5: Data sheet of the 7815 voltage regulator

International
IOR Rectifier

Data Sheet No. PD60147 rev.V

IR2110(S)PbF/IR2113(S)PbF

HIGH AND LOW SIDE DRIVER

Features

- Floating channel designed for bootstrap operation
  Fully operational to +500V or +600V
  Tolerant to negative transient voltage
  dV/dt immune
- Gate drive supply range from 10 to 20V
- Undervoltage lockout for both channels
- 3.3V logic compatible
  Separate logic supply range from 3.3V to 20V
  Logic and power ground ±5V offset
- CMOS Schmitt-triggered inputs with pull-down
- Cycle by cycle edge-triggered shutdown logic
- Matched propagation delay for both channels
- Outputs in phase with inputs

Product Summary

V_{OFFSET} (IR2110)	500V max.
(IR2113)	600V max.
I_O+/-	2A / 2A
V_{OUT}	10 - 20V
$t_{on/off}$ (typ.)	120 & 94 ns
Delay Matching (IR2110)	10 ns max.
(IR2113)	20ns max.

Packages

14-Lead PDIP
IR2110/IR2113

16-Lead SOIC
IR2110S/IR2113S

Description

The IR2110/IR2113 are high voltage, high speed power MOSFET and IGBT drivers with independent high and low side referenced output channels. Proprietary HVIC and latch immune CMOS technologies enable ruggedized monolithic construction. Logic inputs are compatible with standard CMOS or LSTTL output, down to 3.3V logic. The output drivers feature a high pulse current buffer stage designed for minimum driver cross-conduction. Propagation delays are matched to simplify use in high frequency applications. The floating channel can be used to drive an N-channel power MOSFET or IGBT in the high side configuration which operates up to 500 or 600 volts.

Typical Connection

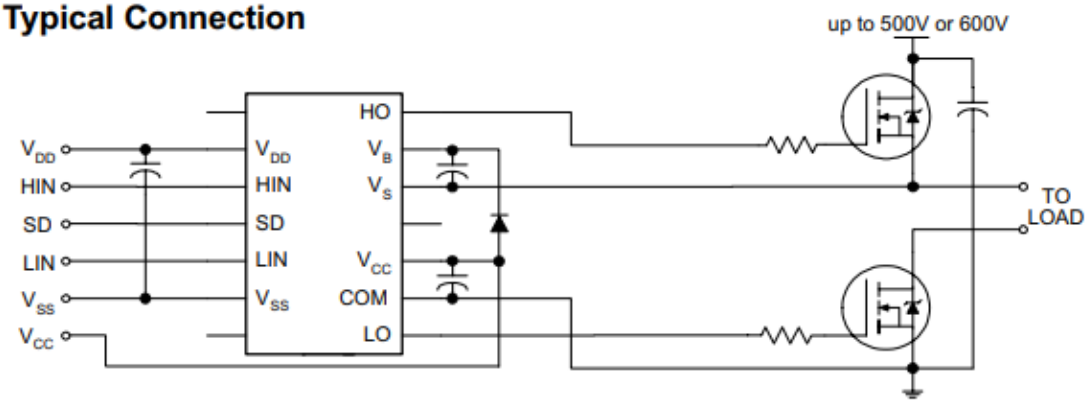

(Refer to Lead Assignments for correct pin configuration). This/These diagram(s) show electrical connections only. Please refer to our Application Notes and DesignTips for proper circuit board layout.

Figure A6: 1st page of the data sheet of the IR2110

Absolute Maximum Ratings

Absolute maximum ratings indicate sustained limits beyond which damage to the device may occur. All voltage parameters are absolute voltages referenced to COM. The thermal resistance and power dissipation ratings are measured under board mounted and still air conditions. Additional information is shown in Figures 28 through 35.

Symbol	Definition		Min.	Max.	Units
V_B	High side floating supply voltage	(IR2110)	-0.3	525	V
		(IR2113)	-0.3	625	
V_S	High side floating supply offset voltage		V_B - 25	V_B + 0.3	
V_{HO}	High side floating output voltage		V_S - 0.3	V_B + 0.3	
V_{CC}	Low side fixed supply voltage		-0.3	25	
V_{LO}	Low side output voltage		-0.3	V_{CC} + 0.3	
V_{DD}	Logic supply voltage		-0.3	V_{SS} + 25	
V_{SS}	Logic supply offset voltage		V_{CC} - 25	V_{CC} + 0.3	
V_{IN}	Logic input voltage (HIN, LIN & SD)		V_{SS} - 0.3	V_{DD} + 0.3	
dV_s/dt	Allowable offset supply voltage transient (figure 2)		—	50	V/ns
P_D	Package power dissipation @ $T_A \leq +25°C$	(14 lead DIP)	—	1.6	W
		(16 lead SOIC)	—	1.25	
R_{THJA}	Thermal resistance, junction to ambient	(14 lead DIP)	—	75	°C/W
		(16 lead SOIC)	—	100	
T_J	Junction temperature		—	150	°C
T_S	Storage temperature		-55	150	
T_L	Lead temperature (soldering, 10 seconds)		—	300	

Recommended Operating Conditions

The input/output logic timing diagram is shown in figure 1. For proper operation the device should be used within the recommended conditions. The VS and VSS offset ratings are tested with all supplies biased at 15V differential. Typical ratings at other bias conditions are shown in figures 36 and 37.

Symbol	Definition		Min.	Max.	Units
V_B	High side floating supply absolute voltage		V_S + 10	V_S + 20	V
V_S	High side floating supply offset voltage	(IR2110)	Note 1	500	
		(IR2113)	Note 1	600	
V_{HO}	High side floating output voltage		V_S	V_B	
V_{CC}	Low side fixed supply voltage		10	20	
V_{LO}	Low side output voltage		0	Vcc	
V_{DD}	Logic supply voltage		V_{SS} + 3	V_{SS} + 20	
V_{SS}	Logic supply offset voltage		-5 (Note 2)	5	
V_{IN}	Logic input voltage (HIN, LIN & SD)		V_{SS}	V_{DD}	
T_A	Ambient temperature		-40	125	°C

Note 1: Logic operational for V_S of -4 to +500V. Logic state held for V_S of -4V to $-V_{BS}$. (Please refer to the Design Tip DT97-3 for more details).
Note 2: When V_{DD} < 5V, the minimum V_{SS} offset is limited to $-V_{DD}$.

Figure A7: 2nd page of the data sheet of the IR2110

Quad Picoampere Input Current Bipolar Op Amp

AD704

FEATURES
High DC Precision
75 μV Max Offset Voltage
1 μV/°C Max Offset Voltage Drift
150 pA Max Input Bias Current
0.2 pA/°C Typical I_B Drift
Low Noise
0.5 μV p-p Typical Noise, 0.1 Hz to 10 Hz
Low Power
600 μA Max Supply Current per Amplifier
MIL-STD-883B Processing Available
Available in Tape and Reel in Accordance with EIA-481A Standard
Dual Version: AD706

APPLICATIONS
Industrial/Process Controls
Weigh Scales
ECG/EKG Instrumentation
Low Frequency Active Filters

CONNECTION DIAGRAMS

14-Lead Plastic DIP (N)
14-Lead CerDIP (Q) Packages

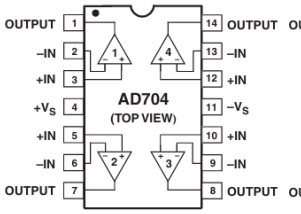

16-Lead SOIC
(R) Package

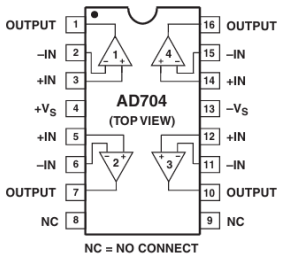

20-Terminal LCC
(E) Package

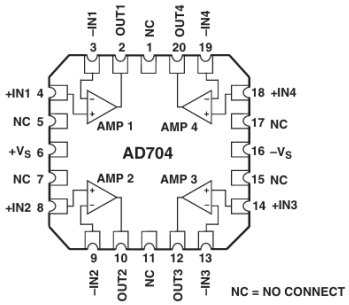

PRODUCT DESCRIPTION

The AD704 is a quad, low power bipolar op amp that has the low input bias current of a BiFET amplifier but which offers a significantly lower I_B drift over temperature. It utilizes super-beta bipolar input transistors to achieve picoampere input bias current levels (similar to FET input amplifiers at room temperature), while its I_B typically only increases by 5× at 125°C (unlike a BiFET amp, for which I_B doubles every 10°C resulting in a 1000× increase at 125°C). Furthermore, the AD704 achieves 75 μV offset voltage and low noise characteristics of a precision bipolar input op amp.

Since it has only 1/20 the input bias current of an AD OP07, the AD704 does not require the commonly used "balancing" resistor. Furthermore, the current noise is 1/5 that of the AD OP07 which makes the AD704 usable with much higher source impedances. At 1/6 the supply current (per amplifier) of the AD OP07, the AD704 is better suited for today's higher density circuit boards and battery-powered applications.

The AD704 is an excellent choice for use in low frequency active filters in 12- and 14-bit data acquisition systems, in precision instrumentation, and as a high quality integrator. The AD704 is internally compensated for unity gain and is available in five performance grades. The AD704J and AD704K are rated over the commercial temperature range of 0°C to 70°C. The AD704A is rated over the industrial temperature of –40°C to +85°C. The AD704T is rated over the military temperature range of –55°C to +125°C and is available processed to MIL-STD-883B, Rev. C.

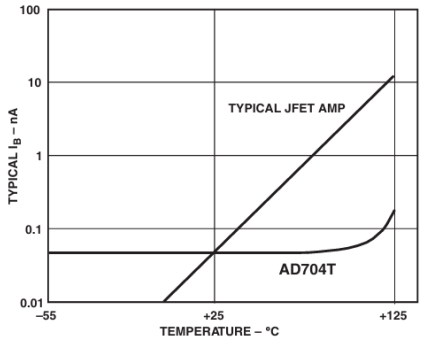

Figure 1. Input Bias Current Over Temperature

REV. C

One Technology Way, P.O. Box 9106, Norwood, MA 02062-9106, U.S.A.
Tel: 781/329-4700 **www.analog.com**
Fax: 781/326-8703

Figure A8: 1st page of the data sheet of the Operational amplifier AD704

AD704–SPECIFICATIONS (@ T_A = 25°C, V_{CM} = 0 V, and ±15 V dc, unless otherwise noted.)

Parameters	Conditions	AD704J/A Min	AD704J/A Typ	AD704J/A Max	AD704K Min	AD704K Typ	AD704K Max	AD704T Min	AD704T Typ	AD704T Max	Unit
INPUT OFFSET VOLTAGE											
Initial Offset			50	150		30	75		30	100	µV
Offset	T_{MIN}–T_{MAX}		100	250		50	150		80	150	µV
vs. Temp, Average TC			0.2	1.5		0.2	1.0			1.0	µV/°C
vs. Supply (PSRR)	V_S = ±2 to ±18 V	100	132		112	132		112	132		dB
T_{MIN}–T_{MAX}	V_S = ±2.5 to ±18 V	100	126		108	126		108	126		dB
Long-Term Stability			0.3			0.3			0.3		µV/month
INPUT BIAS CURRENT[1]	V_{CM} = 0 V		100	270		80	150		80	200	pA
	V_{CM} = ±13.5 V			300			200			250	pA
vs. Temp, Average TC			0.3			0.2			1.0		pA/°C
T_{MIN}–T_{MAX}	V_{CM} = 0 V			300			200			600	pA
	V_{CM} = ±13.5 V			400			300			700	pA
INPUT OFFSET CURRENT	V_{CM} = 0 V		80	250		30	100		50	150	pA
	V_{CM} = ±13.5 V			300			150			200	pA
vs. Temp, Average TC			0.6			0.4			0.4		pA/°C
T_{MIN}–T_{MAX}	V_{CM} = 0 V		100	300		80	200		80	400	pA
	V_{CM} = ±13.5 V		100	400		80	300		100	500	pA
MATCHING CHARACTERISTICS											
Offset Voltage				250			130			150	µV
	T_{MIN}–T_{MAX}			400			200			250	µV
Input Bias Current[2]				500			300			400	pA
	T_{MIN}–T_{MAX}			600			400			600	pA
Common-Mode Rejection[3]		94			110			104			dB
	T_{MIN}–T_{MAX}	94			104			104			dB
Power Supply Rejection[4]		94			110			110			dB
	T_{MIN}–T_{MAX}	94			106			106			dB
Crosstalk[5]	f = 10 Hz										
	R_{LOAD} = 2 kΩ		150			150			150		dB
FREQUENCY RESPONSE											
UNITY GAIN											
Crossover Frequency			0.8			0.8			0.8		MHz
Slew Rate, Unity Gain	G = –1		0.15			0.15			0.15		V/µs
Slew Rate	T_{MIN}–T_{MAX}		0.1			0.1			0.1		V/µs
INPUT IMPEDANCE											
Differential			40‖2			40‖2			40‖2		MΩ‖pF
Common-Mode			300‖2			300‖2			300‖2		GΩ‖pF
INPUT VOLTAGE RANGE											
Common-Mode Voltage		±13.5	±14		±13.5	±14		±13.5	±14		V
Common-Mode Rejection Ratio	V_{CM} = ±13.5 V	100	132		114	132		110	132		dB
	T_{MIN}–T_{MAX}	98	128		108	128		108	128		dB
INPUT CURRENT NOISE	0.1 to 10 Hz		3			3			3		pA p-p
	f = 10 Hz		50			50			50		fA/√Hz
INPUT VOLTAGE NOISE	0.1 to 10 Hz		0.5			0.5	2.0		0.5	2.0	µV p-p
	f = 10 Hz		17			17			17		nV/√Hz
	f = 1 kHz		15	22		15	22		15	22	nV/√Hz
OPEN-LOOP GAIN	V_O = ±12 V										
	R_{LOAD} = 10 kΩ	200	2000		400	2000		400	2000		V/mV
	T_{MIN}–T_{MAX}	150	1500		300	1500		300	1500		V/mV
	V_O = ±10 V										
	R_{LOAD} = 2 kΩ	200	1000		300	1000		200	1000		V/mV
	T_{MIN}–T_{MAX}	150	1000		200	1000		100	1000		V/mV

Figure A9: 2nd page of the data sheet of the Operational amplifier AD704

Voltage Transducer LV 25-P

For the electronic measurement of currents: DC, AC, pulsed..., with galvanic isolation between the primary circuit and the secondary circuit.

16084

I_{PN} = 10 mA
V_{PN} = 10 .. 500 V

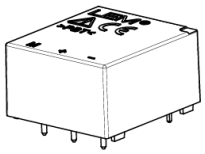

Electrical data

I_{PN}	Primary nominal current rms		10		mA
I_{PM}	Primary current, measuring range		0 .. ± 14		mA
R_M	Measuring resistance		$R_{M\,min}$	$R_{M\,max}$	
	with ± 12 V	@ ± 10 mA_{max}	30	190	Ω
		@ ± 14 mA_{max}	30	100	Ω
	with ± 15 V	@ ± 10 mA_{max}	100	350	Ω
		@ ± 14 mA_{max}	100	190	Ω
I_{SN}	Secondary nominal current rms		25		mA
K_N	Conversion ratio		2500 : 1000		
V_C	Supply voltage (± 5 %)		± 12 .. 15		V
I_C	Current consumption		10 (@ ± 15 V) + I_S		mA

Accuracy - Dynamic performance data

X_G	Overall accuracy @ I_{PN}, T_A = 25°C @ ± 12 .. 15 V		± 0.9		%
	@ ± 15 V (± 5 %)		± 0.8		%
ε_L	Linearity error		< 0.2		%
			Typ	Max	
I_O	Offset current @ I_P = 0, T_A = 25°C			± 0.15	mA
I_{OT}	Temperature variation of I_O	0°C .. + 25°C	± 0.06	± 0.25	mA
		+ 25°C .. + 70°C	± 0.10	± 0.35	mA
t_r	Response time [1] to 90 % of I_{PN} step		40		µs

General data

T_A	Ambient operating temperature		0 .. + 70	°C
T_S	Ambient storage temperature		- 25 .. + 85	°C
R_P	Primary coil resistance	@ T_A = 70°C	250	Ω
R_S	Secondary coil resistance	@ T_A = 70°C	110	Ω
m	Mass		22	g
	Standard		EN 50178: 1997	

Note: [1] R_1 = 25 kΩ (L/R constant, produced by the resistance and inductance of the primary circuit).

Features

- Closed loop (compensated) current transducer using the Hall effect
- Isolated plastic case recognized according to UL 94-V0.

Principle of use

- For voltage measurements, a current proportional to the measured voltage must be passed through an external resistor R_1 which is selected by the user and installed in series with the primary circuit of the transducer.

Advantages

- Excellent accuracy
- Very good linearity
- Low thermal drift
- Low response time
- High bandwidth
- High immunity to external interference
- Low disturbance in common mode.

Applications

- AC variable speed drives and servo motor drives
- Static converters for DC motor drives
- Battery supplied applications
- Uninterruptible Power Supplies (UPS)
- Power supplies for welding applications.

Application domain

- Industrial.

Figure A10: Data sheet of the voltage sensor

Pin Diagrams – PIC16F884/887, 40-Pin PDIP

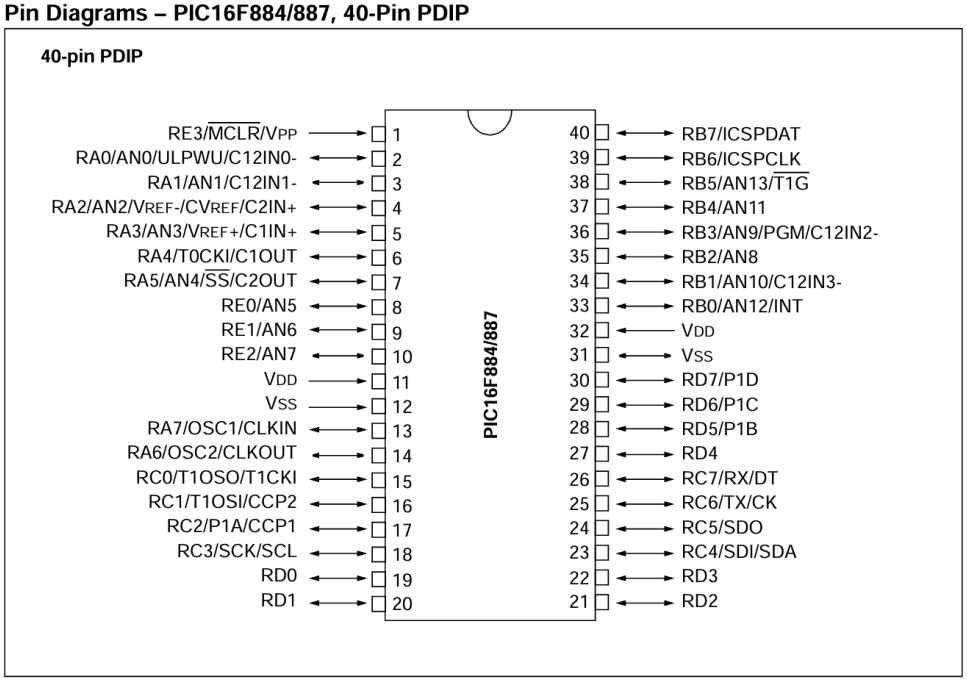

Figure A11: Data sheet of the PIC16F887 microcontroller